



M060070592

# PREPARATION AND CHARACTERIZATION OF RIBAVIRIN NANOCARRIERS TOWARDS IMPROVING THE HEPATITIS C TREATMENT

NWU  
LIBRARY

S MASHA



[orcid.org/0000-0002-5380-7196](https://orcid.org/0000-0002-5380-7196)

Dissertation submitted in fulfilment of the requirements for  
the degree *Master of Science-Chemistry* at the  
North-West University

Supervisor: Dr L KATATA-SERU

Graduation May 2018

Student number: 21949824

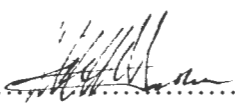
<b>LIBRARY</b>
<b>MAFIKENG CAMPUS</b>
CALL NO.:
2018 -11- 14
ACC.NO.:
<b>NORTH-WEST UNIVERSITY</b>



## DECLARATION

I, Sam Masha, declare herewith that the dissertation entitled, "Preparation and characterization of ribavirin nanocarriers towards improving the Hepatitis C treatment" which I submit to the North-West University as completion of the requirements set for the Master's degree, is my own work and has not already been submitted to any other university.

I understand and accept that the copies that are submitted for examination are the property of the university.

Signature of candidate..........

University number...21949824.....

Signed at ...NWU..... On this 23...day of ...APRIL.....2018.....

## DEDICATION

This dissertation is dedicated to my parents.

## **RESEARCH CONTRIBUTIONS**

S Masha and L Katata-Seru, Preparation and characterisation of ribavirin nanocarriers towards improving Hepatitis C treatment, 7<sup>th</sup> International Symposium on Nanotechnology, Occupational and Environmental Health, 18-21 October 2015, Legend Safari, Limpopo, South Africa (Poster presentation).

## ABSTRACT

The hepatitis C virus (HCV) is among the leading causes of chronic liver diseases worldwide. The current primary treatment for HCV includes the oral administration of ribavirin (RBV) and pegylated interferon alpha (pegasys). The treatment is associated with toxic side effects due to the high daily dosage of 1200 mg RBV and overall low success rate. RBV possess a high accumulation rate in erythrocytes (red blood cells), therefore this makes it difficult for RBV to reach the target cells (hepatocytes) in the liver. The aim of this project was to load RBV into a polymer as nanoparticles (NPs) and characterize their physicochemical properties. The *in vitro* drug release was performed to study the ability of the polymer to release the drug. Eudragit L100 (Eud) and RBV were chosen as polymer and drug respectively. Polyvinyl alcohol (PVA) and poloxamer 407 (POLO) were selected as emulsifying agents.

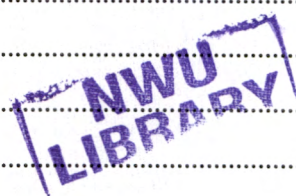
Nanoprecipitation technique was employed to formulate the NPs by varying the surfactant concentration and the type of organic solvent. NPs characteristics such as particle size, polydispersity index (PDI) and zeta potential (ZP) were carried out by Malvern Zetasizer. The effects of surfactant concentration and organic solvent on particle size and ZP were analysed and the two optimised NPs were chosen for further characterisation. The optimised NPs had a diameter ranging from 200-250 nm and ZP of greater than -30 mV. The morphological study of the optimised NPs was carried by scanning electron microscopy and the NPs were spherical.

The Fourier transform infrared spectroscopy showed the major peaks of both drug and polymer. There was clear evidence that there is a high amount of drug entrapped within the polymer. The ultraviolet visible spectroscopy studies showed a high drug encapsulation efficiency of >70%. The drug release studies showed a rapid release within the first 6 hours. The NPs showed the sensitive pH characteristic *in vitro* drug release. The Eud-RBV NPs showed a high thermal stability than pure RBV. The *in vivo* cytotoxicity in *Daphnia magna* showed that NPs were not toxic. Therefore, the use of NPs as drug delivery system for RBV

shows substantial characteristics; this promise a possibility to decrease the high daily intake of RBV thus minimizing its toxic side effects.

# TABLE OF CONTENTS

	Page
DECLARATION .....	
ACKNOWLEDGEMENTS .....	ii
DEDICATION .....	iii
RESEARCH CONTRIBUTIONS .....	iv
ABSTRACT .....	v
LIST OF ABBREVIATIONS .....	x
LIST OF FIGURES.....	xii
page .....	xii
LIST OF TABLES .....	xiv
CHAPTER 1.....	1
INTRODUCTION.....	1
1.1 Background .....	1
1.2 Problem statement .....	5
1.3 Aims and objectives .....	5
1.4 Method of preparation .....	6
1.4.1 Preparation of NPs.....	6
1.4.2 Nanoprecipitation technique.....	6
1.4.3 Selection of polymer .....	8
1.5 Freeze drying process.....	9
CHAPTER 2.....	11
LITERATURE REVIEW .....	11
2.1 Overview of hepatitis .....	11
2.2 Background of HCV .....	12
2.2.1 Structural organization of HCV .....	12
2.2.2 HCV life cycle and replication .....	13
2.3 Nanotechnology and its applications in drug delivery .....	15
2.4 Nanomedicine in the treatment of HCV .....	23
2.4.1 Pegylation of interferon alpha 2a .....	23
2.4.2 Carbon nanotube -based loaded with RBV .....	24
2.4.3 Haemoglobin-RBV conjugates for targeted drug delivery .....	24



2.4.4 Liver-targeting nanoparticles from the amphiphilic random copolymer.....	25
2.4.5 Niosomes containing RBV for liver targeting.....	25
2.4.6 RBV loaded poly(lactide-co-glycolide) nanoparticles .....	26
2.4.7 RBV-Boronic acid loaded nanoparticles .....	26
CHAPTER 3.....	27
METHODOLOGY .....	27
3.1 Materials.....	27
3.2 Development of calibration curve .....	28
3.2.1 Preparation of RBV solution using distilled water.....	28
3.3 Preparation of Phosphate Buffer Saline (PBS).....	28
3.4 Preparation of Simulated Gastric Fluid (SGF) .....	28
3.5 Preparation of Simulated Intestinal Fluid (SIF) .....	28
3.6 Determination of absorbance maxima of RBV .....	29
3.7 Preparation of NPs .....	29
3.8 Evaluation and characterization of Eud-RBV NPs .....	31
3.8.1 Particle size, PDI and zeta potential .....	31
3.8.2 Morphology study of Eud-RBV(PVA) NPs and Eud-RBV(POLO) NPs .....	31
3.8.3 Drug-excipients interaction determination by FTIR .....	31
3.8.4 Crystallinity study of Eud-RBV NPs through XRD.....	32
3.8.5 Encapsulation Efficiency determination.....	32
3.8.6 <i>In vitro</i> drug release analysis.....	32
3.8.7 Thermal analysis of Eud-RBV NPs.....	33
3.8.8 <i>In vivo</i> cytotoxicity study of Eud-RBV NPs .....	33
CHAPTER 4.....	34
RESULTS AND DISCUSSION .....	34
4.1 Calibration curve of RBV.....	34
4.2 Average particle size analysis of Eud-RBV NPs .....	35
4.2.1 Effect of organic solvent in average particle size of NPs.....	36
4.2.1 Effect of surfactant on NPs size analysis .....	37
4.3 Effect of PDI on average particle size.....	38
4.4. Effect of surfactant on Zeta Potential of NPs.....	39
4.5 Selection of optimised NPs .....	42
4.5.1 FTIR analysis .....	42
4.5.2 XRD analysis.....	46



4.5.3 Morphology of Eud-RBV NPs through SEM .....47

4.5.4 Encapsulation Efficiency.....47

4.5.5 Drug release studies .....48

4.5.6 Thermal analysis .....49

**CHAPTER 5 .....54**

**CONCLUSIONS AND RECOMENDATIONS.....54**

**5.1 Conclusions .....54**

**5.2 Recommendations .....54**

**REFERENCES .....55**

## LIST OF ABBREVIATIONS

ATP	Adenosine triphosphate
BSA	Bovine serum albumin
DLS	Dynamic light scattering
DNA	Deoxyribonucleic acid
EA	Ethyl acetate
EE	Encapsulation efficiency
EtOH	Ethanol
Eud	Eudragit L100
Eud-RBV	Eudragit-ribavirin
Eud-RBV(POLO)	Eudragit-ribavirin(poloxamer 407)
Eud-RBV(PVA)	Eudragit-ribavirin(PVA)
FDA	Food and drug administration
FE-SEM	Field emission scanning electron microscopy
FTIR	Fourier transform infrared spectroscopy
GIT	Gastrointestinal tract
HAV	Hepatitis A virus
HBV	Hepatitis B virus
HCV	Hepatitis C virus
HDV	Hepatitis D virus
HEV	Hepatitis E virus
HGV	Hepatitis G Virus
HIV	Human immunodeficiency virus

mRNA	Massenger ribonucleic acid
nm	Nanometre
NPs	Nanoparticles
PBA	Phenylboronic acid
PDI	Polydispersity index
PEG	Polyethylene glycol
POLO	Poloxamer 407
PGA	Poly (glycolic acid)
PVA	Polyvinyl alcohol
RBC	Red blood cells
RBV	Ribavirin
RES	Reticuloendothelial system
RNA	Ribonucleic acid
SDDS	Smart drug delivery systems
SEM	Scanning electron microscopy
siRNA	Small interfering ribonucleic acid
SWCNT	Single welled carbon nanotubes
UV- <i>vis</i>	Ultraviolet visible spectroscopy
WHO	World Health Organisation
ZP	Zeta potential

## LIST OF FIGURES



page

Figure 1.1: Differences between a healthy liver and hepatitis infected liver.....	1
Figure 1.2: Molecular structure of RBV.....	4
Figure 1.3: Illustration of nanoprecipitation method .....	7
Figure 1.4: Molecular structure of Eud.....	8
Figure 2.1: Morphology of HCV.....	13
Figure 2.2: Schematic representation of HCV life cycle.....	14
Figure 2.3: Differences between nanocapsule and nanosphere.....	17
Figure 2.4: Illustration of different mechanisms for drug release.....	22
Figure 3.1: Schematic representation of nanoprecipitation method.....	30
Figure 4.1: Absorbance maxima of RBV in PBS at pH 7.4.....	34
Figure 4.2: Calibration curve of RBV in PBS.....	35
Figure 4.3: Average particle size of NPs prepared varying PVA concentrations in EA and EtOH.....	36
Figure 4.4: Effect of average particle size in various surfactant concentrations using EA .....	38
Figure 4.5: Intensity versus size in all NPs prepared from PVA using EA.....	39
Figure 4.6: Intensity versus size in all NPs prepared from POLO using EA.....	39
Figure 4.7: Eudragit L100 FTIR spectrum.....	43
Figure 4.8: RBV FTIR spectrum.....	43

Figure 4.9: FTIR spectrum for Eud-RBV(PVA) NPs.....44

Figure 4.10: FTIR spectrum for Eud-RBV(POLO) NPs.....45

Figure 4.11: XRD curves for RBV, Eud-RBV(PVA) NPs, Eud-RBV(POLO) NPs  
and Eud.....46

Figure 4.12: SEM images of Eud-RBV(PVA) NPs and Eud-RBV(POLO) NPs.....47

Figure 4.13: Drug release profile of Eud-RBV(PVA) NPs, Eud-RBV(POLO) NPs  
and RBV.....48

Figure 4.14: TGA curves of RBV, Eud, Eud-RBV(PVA) NPs and Eud-RBV(POLO) NPs...50

Figure 4.15: DSC curves f RBV, Eud, Eud-RBV(PVA) NPs and Eud-RBV(POLO) NPs.....51

Figure 4.16: Concentration effect curve showing the influence of the Eud-RBV(PVA) NPs  
On immobility of the introduced *Daphnia magna* as observed after  
24 h.....53

Figure 4.17: Concentration effect curve showing the influence of the  
Eud-RBV(POLO) NPs.....53

## LIST OF TABLES

	page
Table 1.1: Pegasys and RBV dosing recommendations.....	2
Table 2.1: Approved drugs for the treatment of HCV.....	15
Table 2.2: Nanomedicine based therapeutics in clinical use and under investigations.....	20
Table 4.1: Variation of ZP in NPs prepared using EA.....	40
Table 4.2: Variation of ZP in NPs prepared using EtOH.....	41
Table 4.3: TGA results for RBV, Eud, Eud-RBV(PVA) NPs, Eud-RBV(POLO) NPs.....	49
Table 4.4: The results of the probit analysis showing LC <sub>x</sub> for Eud-RBV(PVA) NPs and Eud-RBV(POLO) NPs.....	52

## CHAPTER 1

### INTRODUCTION

#### 1.1 Background

Hepatitis C virus (HCV) became a pandemic treat since its discovery in the late 1980s (Chakravarti *et al.*, 2013). It is known as one of the causes of liver inflammation and reported to be the most prevalent leading to chronic hepatitis (Madigan M.T, 2012). According to World Health Organization (WHO), the statistical data shows the HCV prevalence of over 184 million people that are living with this virus worldwide. Furthermore over half a million lives are claimed every year (Messina *et al.*, 2015) from HCV related diseases. Sub-Saharan Africa is leading in HCV prevalence of an estimated 32 million people that are infected, in which 3 quarters are at risk of developing chronic hepatitis (Karoney & Siika, 2013). HCV is among the leading causes of death in HIV-positive patients who are taking highly active antiretroviral therapy (Shepard *et al.*, 2005).

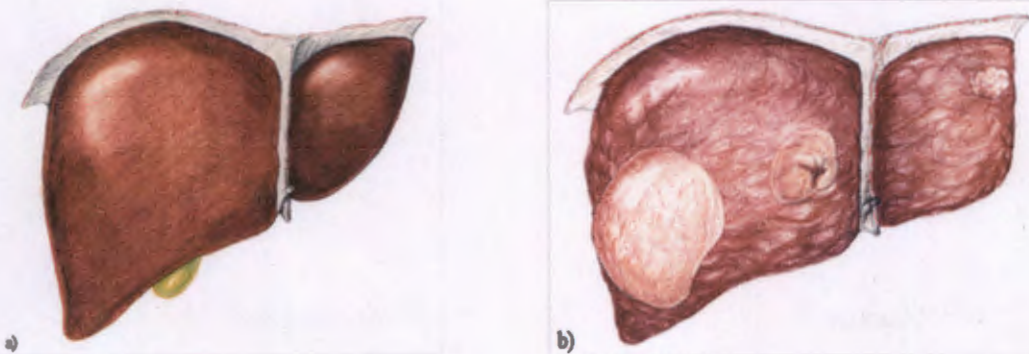


**Figure 1.1:** Differences between (a) healthy liver and (b) hepatitis infected liver ( WHO, 2014)

The virus infects the liver cells called hepatocytes and causes irritation and swelling of the liver (Figure 1.1) (WHO 2014). The infection can range from mild illness lasting for a few weeks and progress to chronicity resulting into more lifelong serious conditions such as

hepatocellular carcinoma, liver cirrhosis and liver cancer (Karoney & Siika, 2013). Worldwide, HCV causes about 57% cases of liver cirrhosis and over 78% of liver cancer (Chakravarti *et al.*, 2013). Most diseases caused by HCV cause have high mortality rate of over 80%, therefore, the virus makes an integral part to the burden of chronic diseases that claim millions of lives (Chakravarti *et al.*, 2013).

HCV consists of four different genotypes that exhibit a high genetic variety characterized by different regions in genotype prevalence (Shepard *et al.*, 2005). Therefore HCV poses a challenge to the development of an effective vaccine and pan-genotypic treatments (Messina *et al.*, 2015).

The current primary treatment for HCV is a combination of intravenous administration of pegasys and orally taken ribavirin (RBV). The two drugs are taken together with one of the secondary line drugs which include, telaprevir, boceprevir, sovaldi or ollysio, depending on the genotype of the virus (Van Vlierberghe *et al.*, 2001; Shepard *et al.*, 2005). The dosage and duration of the treatment varies according to the weight of the patient, progress of the infection and also the genotype of the virus (Table1.1). The treatment has a low success rate of 64% and is associated with adverse side effects which leads to poor patient’s adherence (Takaki *et al.*, 2004).

**Table 1.1:** Pegasys and RBV dosing recommendations (WHO, 2013)

Hepatitis C virus Genotype	Pegasys dose (once weekly)	Ribavirin dose (daily)	Duration
Genotypes 1, 4	180 mcg	<75 kg = 1000 mg	48 weeks
		≥75 kg = 1200 mg	48 weeks
Genotypes 2,3	180 mcg	800 mg	24 weeks



RBV is taken as a tablet, a capsule or as solution twice a day, in the morning and the evening, for 24 to 48 weeks or longer. The daily dosage varies from 800 to 1200 mg depending on the patient's weight. The patients weighing  $\leq 75$  kg take 1000 mg and those weighing  $\geq 75$  kg take 1200 mg together in combination with 180 mcg / 0.5 mL weekly injection of pegasys (WHO, 2013).

The combination therapy can cure the virus in 50% of patients infected with genotype 1 and 80% of patients infected with genotype 2 or 3 (Nishimata *et al.*, 2014). This therapy is usually suggested for vulnerable patients at risk of chronic hepatitis (Oze *et al.*, 2011). The risk is usually defined by measuring RNA level of the virus and liver biopsy that shows a portal fibrous connective tissues along with moderate redness and necrosis (Iwasaki *et al.*, 2006). The treatment has challenges including high drug toxicity, poor bioavailability, poor efficacy and stability (Oze *et al.*, 2011; Kumar, 2013).

Currently there are on-going researches on developing and improving HCV treatment (WHO, 2014). Scientists from various disciplines including, microbiology, virology, medicine, pharmaceuticals and nanotechnology are attempting to solve this problem (Logothetidis, 2012).

In this study, the proposed solution for improving the treatment was through the application of nanotechnology. The technology was used to improve the oral treatment for HCV using RBV as a model drug. Improvement was aimed at protecting the drug against unfavourable conditions within gastro intestinal tract and preventing the side reactions. It also helps in increasing the stability and oral bioavailability of the drug and minimising its adverse side effects by reducing the high daily dosage of 800 -1200 mg RBV. Preparation and characterisation of Eudragi L100 (Eud) and RBV nanoparticles (NPs) was proposed in the study, in order to address some challenges facing HCV treatment such as high dosage, oral bioavailability and adverse side effects. The expected results are improved controlled release over a period of time, thus reducing overall dosage.

RBV was chosen because it is one of the first line drugs in the treatment of HCV and it has been used for years without any modification. Even though it has shown a encompassing spectrum of antiviral action on both DNA and RNA viruses, the raw drug has not been

effective enough to cure liver infections (Reddy *et al.*, 2009). RBV is also used to treat other infections such as respiratory syncytial virus and Lassa fever virus (Crotty *et al.*, 2002). The molecular mechanism of RBV is not yet well known but believed that it inhibits the synthesis of viral nucleic acid and messenger RNA capping (Patterson & Fernandez-Larsson, 1990). The main physicochemical of RBV (Figure 1.2) are: molecular Weight of 244. 207 g/mol, half-life of 298 h and solubility of 142 mg/mL

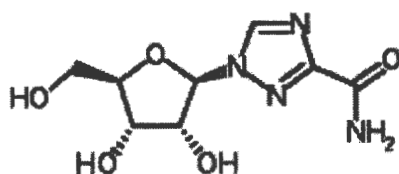


**Figure 1.2:** Molecular structure of RBV (WHO, 2013)

The major limitations of RBV are; haemolytic anaemia may occur with a significant drop in haemoglobin and this may worsen cardiac diseases leading to fatal or nonfatal myocardial infarctions. Risk of hepatic failure and severe hypersensitivity reactions including, urticarial, angioedema, bronchoconstriction, anaphylaxis and severe skin reactions. Pulmonary disorders, severe depression, bone marrow suppression etc (WHO, 2013).

Nanoprecipitation method was used to formulate RBV NPs from Eud polymer. Eighteen NPs were prepared in variation of surfactant concentrations and different organic solvents. The NPs with good particle parameters such as size, polydispersity index (PDI) and zeta potential (ZP) were chosen for further characterisation.

## 1.2 Problem statement

In 2013, WHO estimated that over 150 million people were at risk of developing chronic hepatitis. Meanwhile Sub-saharan Africa has the leading prevalence of HCV with estimated 5.3% and it progresses to chronicity in about 75% of infected individuals in Africa. The co-infection of Human Immunodeficiency Virus (HIV) and HCV increases the risk of chronic liver diseases and Africa has the highest prevalence of HIV as well. The RBV treatment is related with the occurrence of unfavourable events (Patterson & Fernandez-Larsson, 1990; Guo *et al.*, 2015). It is thought to result from the lack of phosphates in red blood cells (RBC), therefore leading into RBV molecules becoming trapped intracellular and accumulate, reading into a very high intra-RBC concentrations that exceed 1mM (Dong *et al.*, 2013). The high intracellular RBV concentrations in RBCs competitively consume ATP levels, which contributes to haemolytic anaemia (Iwasaki *et al.*, 2006). The side effects mostly occur in patients having decreased cardiovascular and pulmonary functions who are less resistant to haemolytic anaemia. The high toxicity of this treatment leads to poor patient's adherence; therefore it is necessary to improve the RBV treatment for HCV so that it becomes more effective.

## 1.3 Aims and objectives

The purpose of this study was to prepare drug loaded RBV/Eud nanoparticles and characterize their physicochemical properties (size, morphology, encapsulation efficiency and surface charge) and control release to reduce the overall dosage of RBV in drug delivery. Oral bioavailability of RBV will be increased in order to improve the treatment for chronic HCV.

The main objectives of the study are to:

- Prepare the drug loaded RBV/Eud nanocarriers using nanoprecipitation method;

- Characterize the nanocarriers in terms of size, encapsulation efficiency, surface charge and morphology using dynamic light scattering (DLS), ultraviolet spectroscopy (UV), scanning electron microscope (SEM) and fourier transform infrared spectroscopy (FTIR) X-ray diffractometer (XRD), Thermogravimetric analysis (TGA) and Differential scanning calorimetry (DSC);
- Study the *in vitro* drug release of the nanoparticles and encapsulation efficiency (EE);
- Determine *in vivo* cytotoxicity test using Daphnia magna modelling assay.

## **1.4 Method of preparation**

### **1.4.1 Preparation of NPs**

There are various methods developed for the formation of polymeric NPs since the era of nanotechnology has arisen (Pillai & Panchagnula, 2001; Reis *et al.*, 2006). In order to successfully develop NPs with desired properties of choice, the technique of NPs formation should be considered (Nagavarma *et al.*, 2012). The widely used methods include; nanoprecipitation, solvent evaporation, salting out, emulsification/solvent diffusion, dialysis and supercritical fluid technology (Pillai & Panchagnula, 2001). These methods are classified into two categories according to whether their formation of NPs involves a polymerization reaction or is achieved directly from a preformed polymer or ionic gelation (Reis *et al.*, 2006; Nagavarma *et al.*, 2012).

### **1.4.2 Nanoprecipitation technique**

Nanoprecipitation method (Figure 1.3) was chosen for the preparation of NPs in this study. This technique is also known as solvent displacement method and was modified by Fessi *et al.* 1989. It involves only one-step nanoprecipitation based on solvent displacement (Morales-Cruz *et al.*, 2012a; Nagavarma *et al.*, 2012; Lepeltier *et al.*, 2014).

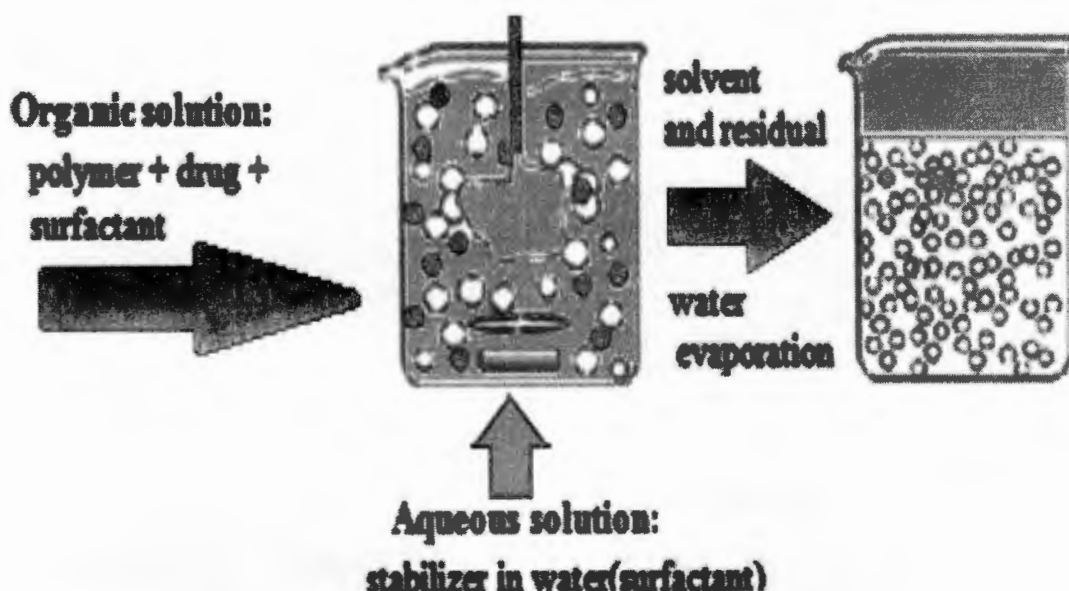


**Figure 1.3:** Illustration of nanoprecipitation method (Nagavarma *et al.*, 2012)

The nanoprecipitation technique is the most commonly used among other methods which account for more than 50% nanoparticles reported for drug delivery ((Reis *et al.*, 2006). This method is easy, straight forward and also able to help the encapsulation of both hydrophilic and hydrophobic drugs into NPs (Pinto Reis *et al.*, 2006; Morales-Cruz *et al.*, 2012b). The nanoprecipitation technique was used to prepare the Eud-RBV NPs. This method involves the precipitation of a dissolved polymer from an organic solution and the dispersion of the organic solvent in the aqueous mixture in the presence or absence of a surface-active agent (Nagavarma *et al.*, 2012).

The first step involves dissolving the polymer in organic solvent of intermediate polarity. This phase is transferred into a stirred aqueous solution containing a stabilizer as a surfactant. The polymer deposition on the surface forming boundary between the water and the organic solvent, caused by fast diffusion of the solvent, results into the instant formation of a NPs. Stirring for a longer period eliminates the organic solvent and then the particles are freeze dried (Nagavarma *et al.*, 2012).

### 1.4.3 Selection of polymer

Polymer selection is a very important fundamental task in the formulation of NPs for drug delivery. The task requires an exhaustive understanding of the surface properties of the polymer that can yield the wanted functions in drug delivery (Pillai & Panchagnula, 2001). There are inherent diversity of polymer structures with different characteristics in which NPs can be prepared from (Nagavarma *et al.*, 2012). The polymer selection is dependent on the need for wide biochemical characterization (Pillai & Panchagnula, 2001).

Polymers are classified into two groups, namely, natural (albumin, chitosan, algenate, etc) and synthetic (poly lactic acid, poly lactide-co-glycolide, Eud etc) (Pillai & Panchagnula, 2001). Synthetic polymers are found in a broad diversity of makeup and their characteristics are readily adjustable. Natural polymers bear from batch to batch diversity due to difficulties in refinement therefore synthetic polymers are often employed in drug delivery (Angelova & Hunkeler, 1999; Pillai & Panchagnula, 2001).

The physicochemical properties of the polymer such as hydrophilicity, surface charge, lubricity, surface energy and smoothness regulate the biocompatibility with cells, tissues and blood (Angelova & Hunkeler, 1999). Moreover they influence the toxicity and physical properties such as permeability, durability and degradability (Nagavarma B V N, 2012). In this study Eud (Figure 1.4) was considered the better polymer for preparation of RBV NPs.

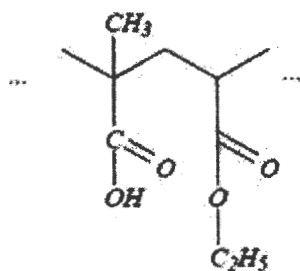


**Figure 1.4:** Molecular structure of Eud



Eudragit polymers are well known in pharmaceuticals and widely used for different NPs as they are biocompatible in nature (Hao *et al.*, 2013). These polymers are classified into synthetic polymers which are frequently used in oral drug delivery systems. They are further classified according to their pH dependence (Aguilar *et al.*, 2015). Eudragit L, S and E are pH-dependent whereas Eudragit RS, RL and NE are pH independent; this is determined by the organic functional groups on the side chains such as carboxylic acid, alcohol or ether (Haznedar & Dortunç, 2004). They can be used with or without other polymers for targeted drug release in desired organ within the GIT (Haznedar & Dortunç, 2004). Among the family of the Eudragits, Eud was chosen because it's an enteric pH-dependent copolymer. It is soluble above pH 5.5 medium and has been commonly used for the preparation of enteric solid dosage forms as good coating and skeleton material (Hao *et al.*, 2013).

The polymer has anionic properties and the surface of RBC is also negatively charged. The 90% of the total charge of RBCs is thought to come from the sialic acid on glycoproteins and glycolipids on the surface. Therefore when developing drugs with anti-hemolysis properties, the surface properties and uptake pathways of RBC should be considered (Guo *et al.*, 2015). This choice of Eud suggests that, there will be repulsion between NPs and RBC, therefore minimise the high accumulation of RBV in RBC.

### **1.5 Freeze drying process**

Freeze drying is a procedure for the smooth drying of high quality products whereby the product is dried by sublimation. It is used as preservation technique in food production industries, e.g. dried fruits, cereals. Another important area of application is the drying of biotechnological and pharmaceutical products, e.g. tissues and tissue extracts, bacteria, vaccines, etc. During this process, the biological properties of the sensitive substances are preserved and the compounds remain unchanged from a qualitative and quantitative point of view.

Freeze-drying is extract water from a product in the frozen state gently. The drying process takes place by the direct transition of a product from the solid phase to the gas phase and the

process occurs under a vacuum. The vapour pressure curve above ice describes the phase transition as a function of the pressure and temperature. The higher the temperature is, the higher the vapour pressure. If the vapour pressure is higher than 6.11 mbar, water passes through all three phases: solid, liquid, and gas. If the vapour pressure is below 6.11 mbar and energy is added, the ice will be directly converted into water vapour once the sublimation curve is reached. If thermal energy is added to pure ice with a temperature of less than  $-30\text{ }^{\circ}\text{C}$  at a pressure of 0.37 mbar, it will be converted into water vapour once it reaches  $-30\text{ }^{\circ}\text{C}$ .

The vacuum prevents the melting of ice when energy is added. If thermal energy is added to a frozen product under vacuum, thawing of the product will be prevented and the water that is contained within the product will be released in the form of water vapour.

## **1.6 Overview of dissertation**

This dissertation comprises of five chapters

**Chapter 1:** Brief introduction of the study including aims and objective.

**Chapter 2:** Reports on the literature about HCV, nanotechnology and its application in attempt to improve the HCV treatment.

**Chapter 3:** Presents the methods for preparation of Eud-RBV NPs and their characterisation.

**Chapter 4:** Deals with results and discussion of data analysis of the research study.

**Chapter 5:** Draws conclusion about the work and findings, including the recommendations for future work.



## CHAPTER 2

### LITERATURE REVIEW

#### 2.1 Overview of hepatitis

Hepatitis is a term defining the irritation and swelling of the liver (WHO, 2013). It is known as the leading cause of liver related diseases worldwide (Chakravarti *et al.*, 2013). There are various causes of hepatitis reported, which include excessive amount of alcohol, toxins and chemicals that are poisonous to human; autoimmune diseases that cause the immune system to attack the healthy tissues in the body and viruses (Madigan *et al.*, 2012). Among all these causes, viral hepatitis is the leading form of hepatitis in the world (WHO, 2013).

Viral hepatitis is caused by the group of infectious viruses that infects the liver cells and affects hundreds of millions of people worldwide (WHO, 2013). There are six known distinct hepatitis viruses that have been identified and named as hepatitis A, B, C, D, E and G (WHO, 2013; Madigan *et al.*, 2013). These viruses differ in terms of their effects, duration of infection, transmission and treatment (Dubuisson & Cosset, 2014a). Furthermore, they consist of different epidemiological profiles (Chakravarti *et al.*, 2013; Dubuisson & Cosset, 2014b).

The Hepatitis B virus (HBV) and HCV have been reported to be the most prevalent, difficult to treat and hence leading to chronic hepatitis (WHO, 2013; Madigan *et al.*, 2012). According to the WHO, it is estimated that about 600 000 and 350 000 people die every year from HBV and HCV respectively. This is because viral hepatitis is a latent epidemic and most people are not aware of their infection (WHO, 2013). The Global Burden of Disease reported that HBV and HCV together caused over 1.4 million cases of deaths in 2010 worldwide, including those from acute infections, cirrhosis and liver cancer (WHO, 2013).

Hepatitis A virus (HAV) and hepatitis E virus (HEV) also cause millions cases of acute illness every year, which can last for several months. Hepatitis D virus only causes problems

in people infected with HBV, since it cannot survive on its own because it requires a protein that is produced by HBV to enable it to infect liver cells (Messina *et al.*, 2015). Hepatitis G virus (HGV) has been discovered recently and found to resemble HCV; the epidemiology of the virus is undergoing investigations at present and some investigators do not recognize it as a cause of hepatitis (WHO, 2013).

Transmission routes of viral hepatitis are different. The exposure to infected blood through blood transfusion and unsterile injection practices serve as a major route for the spread of HBV and HCV. Infection from mother to unborn child during pregnancy and delivery serves as the secondary route for HBV, HCV and HGV (WHO, 2013; Shepard *et al.*, 2013; Madigan *et al.*, 2012). Consumption of contaminated food and water serves as a potential transmission route for HAV and HEV.

The cure and vaccination are available for some types of viral hepatitis, including HAV and HBV. Some acute hepatitis viruses such as HDV, HGV and HEV last for a few weeks and can be cleared from the body by the immune system or by taking simple over counter medicines such as paracetamol (WHO, 2013). However, the major challenge is the treatment and prevention of chronic HCV. This virus consists of four genotypes named 1,2,3 and 4 which differ in some characteristics such as virulence and stability, therefore it is difficult to design the best vaccine for HCV (Kumar, 2013)

## **2.2 Background of HCV**

### **2.2.1 Structural organization of HCV**

The morphology of this virus is that; it is 50 nm in diameter, enveloped with proteins (E1 and E2), single stranded RNA positive sense (Figure 2.1) (Dubuisson & Cosset, 2014b). It is classified as a separate genus (Hepacivirus) the member of the family, *Flaviviridae*. Its genotypes vary in their impact, virological response, epidemiology and the strains belonging to different genotypes differ at 30-35% of nucleotide sites (Messina *et al.*, 2015).

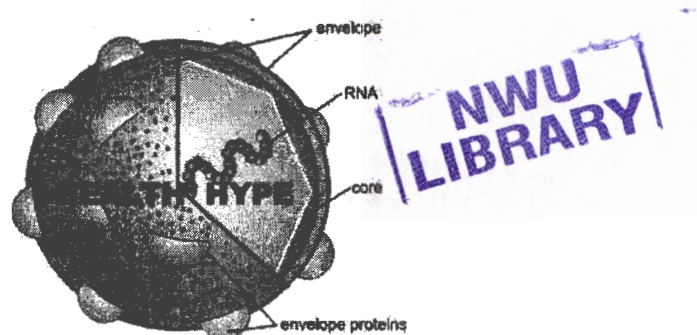


**Figure 2.1:** Morphology of HCV (WHO, 2014)

The reservoir of the virus is human, but it can also infect chimpanzees, resulting in the same effects as in humans (WHO, 2013; Madigan *et al.*, 2012).

### **2.2.2 HCV life cycle and replication**

The viral attachment to the host cell is mediated by the proteins on the envelope. The proteins play a significant part in the receptor binding mechanism and the fusion process between the endosomal host cell membrane and viral envelope (Figure 2.2 stage 1) (Dubuisson & Cosset, 2014a). The nucleocapsid is then released into the cytoplasm of the host cell (Figure 2.2 stage 2) as a result of a merger between cellular and viral membranes (Pawlotsky *et al.*, 2007).

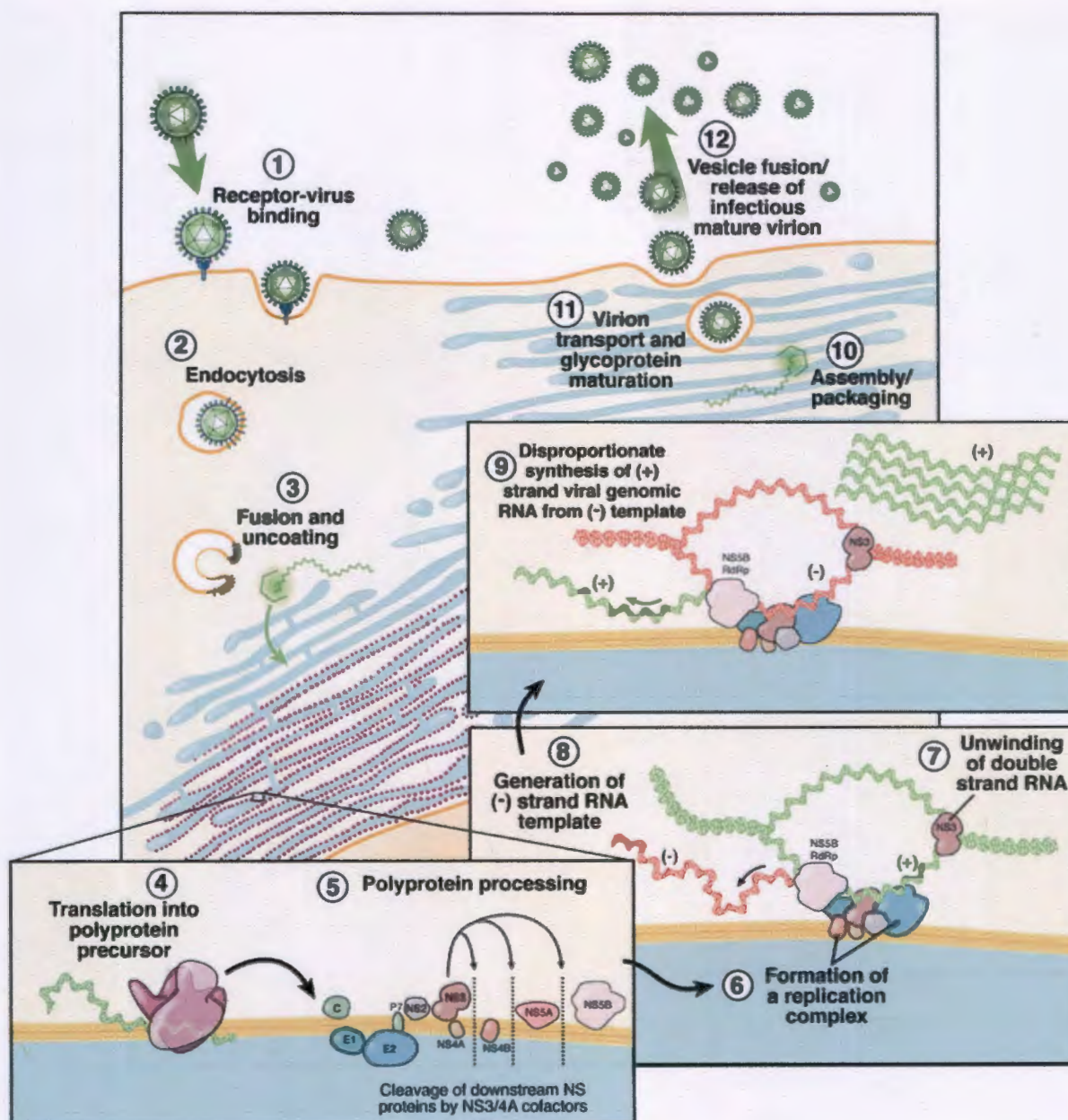


**Figure 2.2:** Stage by stage representation of HCV life cycle (Pawlotsky *et al.*, 2007)

The nucleocapsid of the virus releases free positive strand genomic RNA into the host cell cytoplasm (Figure 2.2 stage 3). The liberated RNA and newly formed RNA serve together as messenger RNA (mRNA) for formation of the viral polyprotein (Dubuisson *et al.*, 2008). Figure 2.2 represents a stage by stage life cycle of HCV from entrance to replication within host cell. Every stage of replication of this virus presents a potential target for antiviral therapy. The different classes of drugs target different stages (Pawlotsky *et al.*, 2007). Table 2.2 briefly illustrates the current drugs used to treat HCV with their targeted site of action during the replication of this virus.



**Table 2.1:** Approved drugs in use for the treatment of HCV

Class	Target of action	Drug	Adult dosage (mg)
Nucleoside analogue	Stop RNA synthesis and mRNA	Ribavirin	800-1200 daily
Protease inhibitors	Stop viral replication	Telaprevir Boceprevir Pariitaprevir	800
Polymerase inhibitor	Blocks RNA polymerase NS5A(5)	Sovaldi(sofosbuvir) Ledipasvir	400 daily
Interferons	Stop RNA capping	Pegasys Peglum	180 mg weekly

Every stage of the HCV life cycle presents a diversity of potential targets for different antiviral drug (Pawlotsky *et al.*, 2007). The nucleoside analogue drugs stop the generation of negative strand RNA template, (Figure 2.2 stage 8). Polymerase inhibitors prevent the assembly of mature RNA from forming a virion, stage 10.

### 2.3 Nanotechnology and its applications in drug delivery

The development and application of nanotechnology in drug delivery has gained attention in recent years. In pharmaceuticals, this technology is aimed at formulating agents into biocompatible nanocarriers to improve their clinical effects (Jain, 2012). The exploitation and use of nanotechnology in presently discovered drugs may modify their clinical therapeutic effects, and minimize the need for discovery and development of new drugs with better properties (Jain, 2012).

The developed nanocarriers are used as drug carrier platforms for targeted, repeated drug applications, resulting in long lasting therapeutic effects (Jain, 2012). There are various types of nanocarriers currently used in drug delivery systems, including gold NPs, lipoparticles, micelles, polymeric NPs, dendrimers, nanofibers, nanoconjugates, liposomes, solid lipid NPs, etc. (Logothetidis, 2012; Gao *et al.*, 2014).

The preparation and loading of therapeutic agents into NPs has proved the following successful achievements (Lembo & Cavalli, 2010b):

- The enhancement of the solubility and absorption of hydrophobic drugs;
- Delivery of drugs into target areas in the body;
- The increase in cellular uptake of drugs through compact epithelial and endothelial obstructions;
- Efficient delivery of large molecular drugs such as peptides, nucleic acids and proteins to intracellular sites and
- Delivery of more than two drugs using the same carrier; and follow the same drug delivery route in the body (Lembo & Cavalli, 2010b).

The most commonly used nanocarriers are polymeric nanoparticles (Kumari *et al.*, 2010). These particles are prepared from polymers that act as vehicles for sustained delivery of different therapeutic agents including both high molecular and low molecular weight compounds to target cells and organs (Panyam & Labhasetwar, 2003). There are various types of PNPs, including nanocapsules and nanospheres (Figure 2.3). The immediate proximity of oil in the nanocapsules results into a vesicular structure while its absence in nanospheres provides a matrix organization of the polymeric chains. Considering the encapsulation mechanisms, the drug can be entrapped, dispersed, dissolved within or adsorbed on the nanoparticles (Figure 2.3) (Guterres *et al.*, 2007). They are all nanometer-sized which promotes effective permeation through cell membranes and stability in the blood stream (Nagavarma *et al.*, 2012).

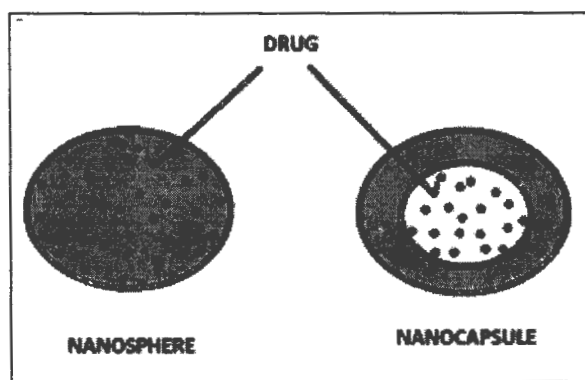


**Figure 2.3:** Difference between nanocapsule and nanosphere (Nagavarma B V N, 2012)

There are various types of delivery systems employed in nanotechnology. Smart drug delivery systems (SDDSs) are also called stimuli-sensitive delivery systems. These are polymers that are environmentally sensitive. They demonstrate sharp changes in behaviour with reaction to an environmental stimuli such as temperature, pH, salts, solvents, electrical field, and biochemical or chemical agents (Kopeček, 2003). SDDSs are founded on the release-on-demand scheme that allows a drug carrier to release a therapeutic drug. This liberation occurs only when it is required in reaction to a specific stimulation (Kopeček, 2013). These systems occur when the polymer configuration in solution is determined by both the polymer–polymer and polymer–solvent interactions (Gao *et al.*, 2014). In an effective solvent, polymer–solvent interactions prevail and the polymer chains are at ease due to minimal inter-segmental reciprocal actions. Whereas in a poor solvent, the polymer will conglomerate due to a unfree chain movement because of increased interactions in polymer–polymer (Kumari *et al.*, 2010).

The other systems in use include the liposomes. These are oily organic macromolecules with homocentric vesicles in which an aqueous volume is entirely enclosed in a lipid bilayer comprised mainly of phospholipids and cholesterol (Lembo & Cavalli, 2010a). Gregoriadis proposed that liposomes are the first vesicular carriers used in drug delivery systems (Guterres *et al.*, 2007). This system has been employed in the treatment of hepatitis. Recently, several notable cationic liposomal anti-HBV siRNA delivery systems have demonstrated potential for the treatment of HBV infections through the incorporation of specific functional moieties (Li *et al.*, 2010). The liposomes can differ in size, from 20- 30

nm in diameter up to micrometres, depending on their chemical makeup and the technique used for preparation (Lembo & Cavalli, 2010a). They can be grouped as either small or large unilamellar vesicles depending on their structures. Their permeability plays a significant role in the encapsulation of both hydrophilic and lipophilic drugs within the lipid bilayer of the liposome (Lembo & Cavalli, 2010a; Eloy *et al.*, 2014). The lipid bilayer in the liquid crystalline phase is more permeable to the encapsulated drug than the gel state (Eloy *et al.*, 2014).

The widely employed systems are NPs. They encapsulate the drug into a polymer membrane and protect it from the undesired conditions within the gastrointestinal tract (GIT). NPs are formulated with biocompatible materials and they have good potential in delivering drugs in a more particular fashion. They deliver the drug either passively by improving the physicochemical properties of the drug carriers such as surface properties and size, or actively by employing tissue/cell particular orienting ligands which permit the targeting of the disease site, while reducing side-effects. NPs delivery systems offer the following several advantages over conventional therapy: (Kumar, 2013; Giannitrapani *et al.*, 2014b; Giannitrapani *et al.*, 2014a):

- Protection of the drug, such as nucleic acid, against deactivation until it get through the target site of action;
- The practicability of encapsulation of both hydrophilic and hydrophobic drugs;
- Developing of pharmacological strength such as increased bioavailability of the agent;
- The reduction of drug concentration fluctuations in the blood hence lower risk of ineffective or toxic concentration;
- Sustained drug release, and;
- Active targeting due to the hypothesis of achieving a good attraction of the nanoparticle system for particular tissues.

The stereotypical NPs are easily opsonized by plasma proteins after systemic administration and recognized as foreign bodies. NPs are then captured by the reticuloendothelial system (RES). The liver and the spleen are the major organs of accumulation of NPs due to their rich



blood supply and the abundance of tissue-resident phagocytic cells, therefore liver targeting by NPs may be favourable for treating liver diseases (Moghimi *et al.*, 2001).

The physicochemical properties of both drug and polymer play a significant role in determining their interactions. Polymer and drug compatibility is known as one of the key factors in determining the effectiveness of polymeric delivery systems (Liu *et al.*, 2004). Size of the NPs determines their absorption and performance into the blood stream. These particles have, in general relatively, higher intracellular uptake compared to microparticles (Panyam & Labhasetwar, 2012). The uptake and distribution of NPs depend on their size (Giannitrapani *et al.*, 2014b). NPs with a mean diameter > 400 nm are quickly captured by the RES and NPs with a diameter < 200 nm show prolonged blood circulation and a relatively low rate of RES uptake. On the other hand, to reduce opsonisation by blood proteins and to prolong bloodstream circulation by limiting RES uptake and reducing immunogenicity/ antigenicity, biologically inert hydrophilic polymers, such as poly(ethylene glycol) (PEG), have been covalently linked to the nanocarrier surface (Owens Iii & Peppas, 2006).

In general, even the new discovered conventional chemotherapeutics for treating cancer diseases still suffer the following limitations in clinical use (Couvreur & Vauthier, 2006):

- Drug resistance at the tumour level because of physiological barriers (noncellular-based mechanisms);
- Drug resistance at the cellular level (cellular mechanisms);
- Distribution, biotransformation and clearance of anticancer drugs in the body.

**Table 2.2:** Nanomedicine based therapeutics in clinical use and under investigations (Sun *et al.*, 2014)

Trade name	Formulation	Drug	Application	Phase of Development
Abraxane	Albumin-bound	Paclitaxel	Metastatic breast cancer	Approved
Caelyx	PEGylated liposome	Doxorubicin	Metastatic breast cancer and ovarian cancer, Kaposi sarcoma	Approved
DaunoXome	Liposome	Daunorubicin	Kaposi sarcoma	Approved
Depocyt	Liposome	cytarabine	Lymphoma	Approved
Doxil	Liposome	Doxorubicin	Kaposi sarcoma	Approved
Genexol-PM	Polymeric micellar	paclitaxel	Breast cancer	Approved
Marqibo	Liposome	Vincristine sulphate	Lymphoblastic leukemia	Approved
Zinostatin stimalamer	Poly(styrene-co-maleic acid)-conjugated neocarzinostatin	Neocarzinostatin	Hepatocellular carcinoma	Approved
Genexol-Polymeric	Methoxy PEG-PLA	paclitaxel	Ovarian and lung cancer	Phase II

Micelles				
CRLX101	Cyclodextrin-PEG micelle	Camptothecin	Ovarian and rectal cancer	phase I/II
CYT-6091	Gold	Tumor necrosis factor alpha	Pancreatic cancer, melanoma, soft-tissue sarcoma, ovarian, and breast cancer	Phase I/III
TKM-080301	Lipid	SiRNA	Liver cancer	Phase I
Docetaxel-PNP	Polymeric	docetaxel	Advanced solid malignancies	Phase I
DEP-Docetaxel	Dendrimer	docetaxel	Breast, prostate, lung and ovarian cancer	Phase I

Encapsulating drug molecules inside NPs allows for controlled drug release. This offers various advantages over the conventional dosing forms based on free drug (Sun *et al.*, 2014). The release characteristics of polymeric NPs are one of the most important features in polymer-drug NPs because of the proposed application in sustained drug delivery systems. There are many factors that affect the release rate of the encapsulated drug (Hans & Lowman, 2002).

There are various drug release mechanisms that have been developed to achieve temporal distribution of drug controlled release using polymers (Uhrich *et al.*, 1999). The purpose of controlled release systems is to maintain an adequate drug concentration in the blood for delivery into target cells or tissues at a desired value as long as possible (Raval *et al.*, 2010). The controlled drug release mechanisms can be classified based on release of drug from nanocarriers. These mechanisms involve diffusion, degradation, swelling followed by diffusion and active efflux (Figure 2.4). All these mechanisms employ physical transformation of constituents involved in the system when they are put into a biological environment (Raval *et al.*, 2010).

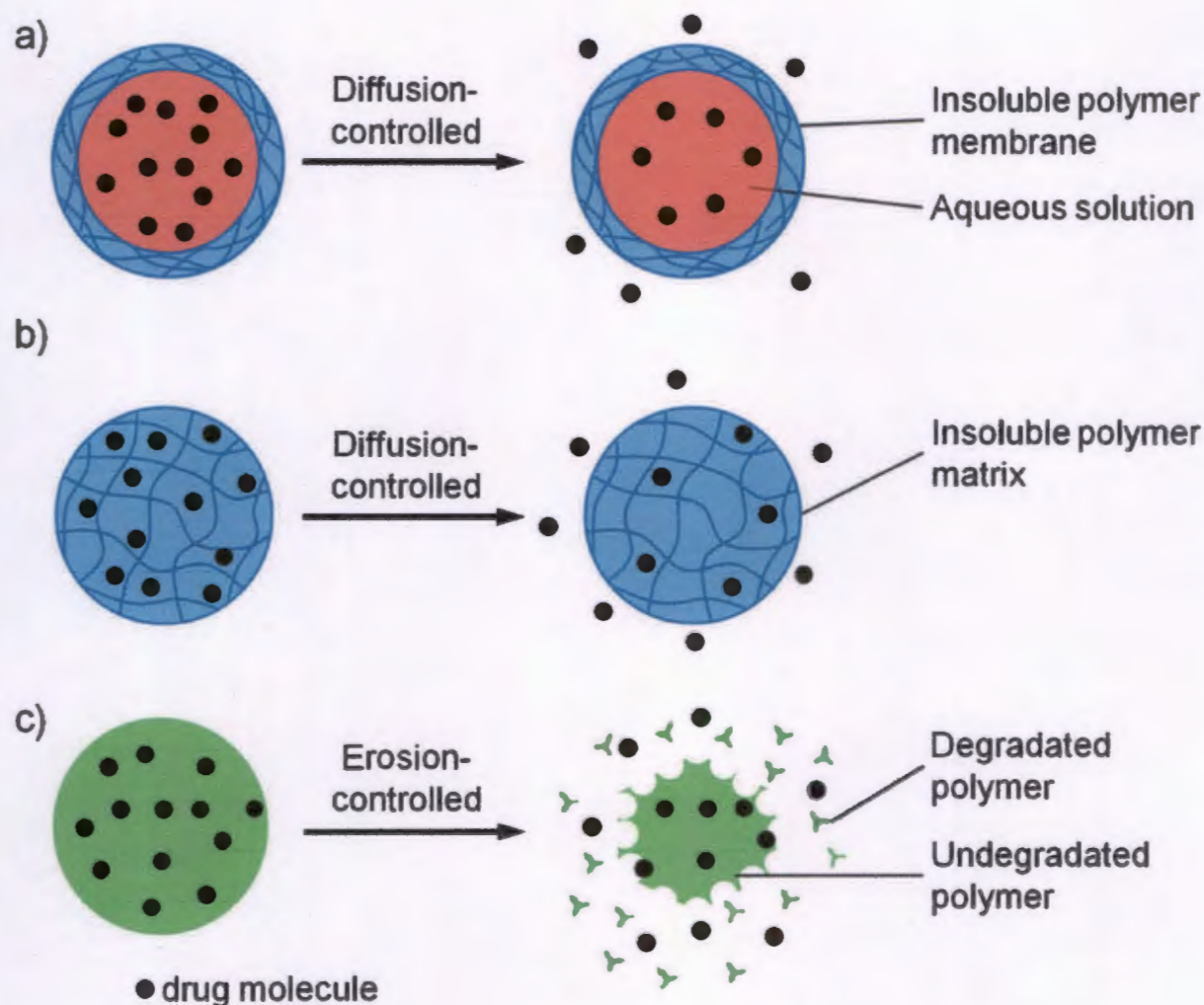


**Figure 2.4:** Illustration of different mechanisms for drug release (Sun *et al.*, 2014)

Many different mechanisms have been developed to attain the controlled release of drugs. This multifariousness of mechanisms is essential influence in different drugs imposing several restrictions on the type of nanocarriers used (Uhrich *et al.*, 1999). For example, a drug that is intended to be released within a given period in stomach where the pH is acidic and environmental conditions waver broadly, will require a controlled release system very different from that of a drug that is to be delivered in a pulsatile manner within the blood system (Uhrich *et al.*, 1999). An essential consideration in designing polymers for any controlled release mechanism is the destiny of the polymer after drug release. Most of the polymers that are naturally excreted from the body are suitable for many controlled release applications (Langer, 1993). These polymers may be excreted directly via the kidneys or may be biodegraded into smaller molecules that are then excreted. Nondegradable polymers could



be employed for parenteral administration, for example PEG is hydrophilic block of wide variety of nanocarriers developed. Moreover for oral applications in which the polymer passes through the gastrointestinal tract (Uhrich *et al.*, 1999).

## **2.4 Nanomedicine in the treatment of HCV**

### **2.4.1 Pegylation of interferon alpha 2a**

Interferon alpha 2a is the current treatment for HCV and is one of the protein drugs susceptible to enzyme degradation and rapid clearance. Therefore, in order to be effective, it needs to be administered frequently to provide consistent serum concentrations within the therapeutic range. Then the interferon alpha was modified by pegylation. This refers to the covalent attachment of PEG to proteins (Abuchowski *et al.*, 1977).

Pegylated interferons are related with increased half-life that contributes to greater biological activity, decreased clearance and lesser antigenicity (Berak *et al.*, 2014). There are two forms of pegylated interferon approved by FDA: peginterferon alfa-2a and peginterferon alfa-2b; both are administered in combination with RBV. They differ in their size, binding and structure of PEG. Peginterferon alfa-2a has a 40 kD PEG molecule that is covalently bound to the protein via lysine. Peginterferon alfa-2b has a 12 kD PEG molecule that is bound by an ester linkage to histidine (Berak *et al.*, 2014). Pegylation is recognized as a promising method for increasing therapeutic efficacy of medicines in clinical settings (Roberts *et al.*, 2002). The group explained the main advantages of pegylation, as an increase in the size of molecule, resulting in reduced filtration by kidneys, an increase in solubility and protection from enzymatic digestion and recognition by antibodies. A variety of molecules, such as small molecules, peptides, proteins, enzymes, antibodies and their fragments, and nanoconjugates have been modified with PEG (Abuchowski *et al.* , 1977 & Roberts *et al.*, 2002 ).

#### 2.4.2 Carbon nanotube -based loaded with RBV

Zhu *et al* 2015 formulated a functionalized single walled carbon nanotubes (SWCNTs) loaded with RBV to develop the treatment for viral diseases in fish especially a grass carp reovirus. The diameter and length distribution of well-dispersed preparations of SWCNTs were measured by FE-SEM. The length and diameter of individual SWCNT were 0-1000 nm and 0.8-1.6 nm (inner diameter), respectively. The percentage content of RBV, BSA and SWCNTs were 20.4%, 41.9%, and 37.7% in RBV-SWCNTs, respectively. The *in vivo* results showed increasing RBV intake was observed by SWCNTs carrier and therapeutic dosage to kill grass carp reovirus was significantly reduced. At 12 days post infection, survival rate and infection rate were 29.7% and 50.4% for naked RBV treatment group exposed to the highest concentration (20 mg/L); however, survival rate of 96.6% and infection rate of 9.4% were observed in 5 mg/L ribavirin-SWCNTs treatment group. In addition, the drug detention time in different organs and tissues (blood, gill, liver, muscle, kidney and intestine) was also significantly extended (about 72 h) compared with the same dosage in naked RBV treatment group (Zhu *et al.*, 2015).

#### 2.4.3 Haemoglobin-RBV conjugates for targeted drug delivery

Brookes *et al.* 2006 developed a novel drug targeting strategy using haemoglobin (Hb) as a natural carrier to target the delivery of RBV to the liver by taking advantage of the natural Hb clearance pathways. Hb is the most abundant blood protein consisting of alpha and beta chains. The main function of Hb is to bind oxygen in the lungs for delivery to respiring tissues in the body and returns carbon dioxide from tissues back to the lungs. The conjugate complex haptoglobin, Hp-Hb-RBV, was selectively taken up *in vitro* by cells that express the Hb-Hp receptor. The recovered ribavirin enzymatically cleaved from Hb-RBV showed equipotent anti-proliferative activity compared to the controlled unconjugated RBV against human liver cell lines. They anticipated that as a protein-drug conjugate Hb-RBV, would be administered intravenously. Furthermore, Hb-RBV may serve as a more potent source of RBV that is particularly suited to acute stages of viral infection or the prevention of HCV recurrence following liver transplant when free RBV cannot be used due to the unacceptably high toxicity (Brookes *et al.*, 2006).

#### 2.4.4 Liver-targeting nanoparticles from the amphiphilic random copolymer

Liver-targeting drug-conjugate nanoparticles were prepared via self-assembly of the lactose-functionalized amphiphilic random copolymer (Li *et al.*, 2008). The functional drug containing amphiphilic random copolymer was prepared using the two-way step chemo enzymatic synthetic route. Particle morphology was spherical with a diameter of  $174 \pm 27$  nm. *In vitro* drug release was studied by dialysis experiments. The concentration of ribavirin released from the copolymer in different media was determined by UV-vis spectroscopy at 207 nm and results showed that raw RBV was quickly released and the cumulative released amount was up to 100% after two hours. Comparatively, RBV was slowly released from drug-conjugate with pseudo zero order kinetics in two different media. The cumulative release was 63 and 38% after seven days (Li *et al.*, 2008). The lower critical aggregation concentration value of 0.1 mg/L of the nanoparticles allowed their use in very dilute aqueous media such as body fluids. Moreover, the nanoparticles had effective growth inhibitory activity in hepG2 human hepatoma cells.

#### 2.4.5 Niosomes containing RBV for liver targeting

The study of Hashim *et al.* 2010 formulated and evaluated RBV encapsulated niosomes for their *in vitro* and *in vivo* characteristics in an attempt to provide a maximum concentration of RBV in the liver by niosomal encapsulation of the drug (Hashim *et al.*, 2010). RBV niosomes were prepared by the thin film hydration method. Their work was aimed at improving the efficacy of low doses of the drug and minimizing the risk of haemolytic anaemia associated with higher doses of the drug. The average particle size showed a narrow size distribution ranging from 0.85-1.01  $\mu\text{m}$ . The calculated PDI of all niosomal NPs ranged from 0.171-0.280. The formulated niosomes appeared as large unilamellar vesicles with spherical shape. Their results showed that the mean RBV concentration in the liver after 4 hours of administration of a single dose for niosomal RBV dispersion was much higher than that obtained from free RBV solution by approximately 6-fold (Hashim *et al.*, 2010). The PDI obtained ranged from 0.171-0.288 and EE ranged from 4.89-4.40%.

#### **2.4.6 RBV loaded poly(lactide-co-glycolide) nanoparticles**

Kumar developed and characterized the RBV loaded poly (lactide-co-glycolide) nanoparticles by double emulsification method to improve the oral delivery of RBV. The morphology of particles was spherical with diameter ranging from 340.0-490.9 nm with high PDI ranging from 0.45-0.94. The zeta potential showed unstable particles with values from -6.51 to -13.30 mV in all five NPs. In his study, the highest drug loading was found to be about 12.19% with an encapsulation efficiency of about 88%. Samples were kept for variable specific periods of time up to 75 days. RBV was released in a sustained manner over a longer period of time of 75 days and around 78% of the drug was released (Kumar, 2013).

#### **2.4.7 RBV-Boronic acid loaded nanoparticles**

Abo-zeid *et al.* 2013 used phenylboronic acid (PBA) and 4-butoxy-3,5-dimethylphenylboronic acid (BPBA) to modify RBV, they used poly (glycerol-adipate) [PGA] polymer to prepare the nanoparticles (RBV-PGA, RBV-PBA20%-C<sub>18</sub>PGA, RBV-PBA20%-C<sub>8</sub>PGA, RBV-BPBA20%C<sub>18</sub>PGA, RBV-BPBA40%-C<sub>8</sub>PGA and RBV-BPBA20%-C<sub>8</sub>PGA) by nano-precipitation method. The particle size ranged from 85-269 nm in diameter for different RBV NPs. The results from <sup>1</sup>H-NMR analysis showed the purity of RBV boronic ester pro-drugs and % yield of RBV-PBA and RBV-BPBA was 77% and 69% respectively. RBV-BPBA-20%C<sub>8</sub>PGA nanoparticles showed an enormous increase of RBV loading% around 1700 times of RBV-PGA (Abo-Zeid *et al.*, 2013).



## CHAPTER 3

### METHODOLOGY

This chapter give detailed experimental review of NPs preparation and characterisation

#### 3.1 Materials

Chemicals	Supplier
Ribavirin	Leapchem (China)
Eudragit L100	Evonik industries (Germany)
Poloxamer 407	Sigma (Johannesburg)
Poly Vinyl Alcohol (PVA)	Sigma (Johannesburg)
Potassium chloride	Sigma (Johannesburg)
Sodium hydrogen phosphate	Sigma (Johannesburg)
Potassium hydrogen sulphate	Sigma (Johannesburg)
Sodium hydroxide	Sigma (Johannesburg)
Sodium chloride	Sigma (Johannesburg)
Acetone	Merck (Johannesburg)
Ethyl acetate	Classworld (Johannesburg)
Hydrochloric acid	Classworld (Johannesburg)

## **3.2 Development of calibration curve**

### **3.2.1 Preparation of RBV solution using distilled water**

Stock solution of 1000 ppm was prepared by dissolving 0.1 g RBV in distilled water to make 1000 mL solution. The eight aliquots of different concentrations from 0 ppm to 35 ppm were prepared from the stock solution.

### **3.3 Preparation of Phosphate Buffer Saline (PBS)**

The following were dissolved in 800 mL of distilled water: 8 g sodium chloride (NaCl), 0.20 g potassium chloride (KCl), 1.44 g sodium hydrogen phosphate ( $\text{Na}_2\text{HPO}_4$ ), 0.24 g Potassium hydrogen phosphate ( $\text{KH}_2\text{PO}_4$ ). NaOH (0.2M) was used to adjust the pH to 7.40. The volume was then filled to 1000 mL with distilled water.

### **3.4 Preparation of Simulated Gastric Fluid (SGF)**

Weighed 2 g of NaCl, 3.2 g of pepsin and added 7 mL HCl to dissolve the salts. The solution was then added into 1000 mL volumetric flask containing about 800 mL of distilled water then filled to the mark with distilled water and adjusted the pH to 1.2 (Marques *et al* 2011)

### **3.5 Preparation of Simulated Intestinal Fluid (SIF)**

Weighed 6.8 g of monobasic  $\text{KPO}_4$  into 500 mL beaker and dissolved it with 250 mL of distilled water. Added 77 mL of 0.2 M NaOH and transferred the solution into 1000 mL volumetric flask. About 1 g of pancreatine was added into the solution and adjusted the pH to 4.6 and filled the flask to the mark with distilled water (Marques *et al* 2011)

### 3.6 Determination of absorbance maxima of RBV

RBV was first dissolved in distilled water and scanning was done in the range of 200-400 nm using (Spectroquant Prove 300, Germany) UV *vis* to determine the absorption maxima of the drug.

### 3.7 Preparation of NPs

NPs were prepared from nanoprecipitation technique using three organic solvents namely, acetone, ethyl acetate (EA) and ethanol (EtOH) to dissolve the polymer. RBV of 50 mg and 100 mg Eud were dissolved in 20 mL beaker containing 10 mL organic solvent under stirring. The organic mixture was transferred drop wise using a syringe equipped with a needle into 20 mL of distilled water containing surfactant with different concentrations (0.25, 0.5 ,0.75, 1.0 , 1.5% PVA or POLO under high stirring speed of 6 000rpm using (Onmi PDH, US) homogenizer for 10 minutes. The solutions were left to stir for 12 h under fume hood using (IKA RT10 Power 10-position magnetic hot plate, Germany) to evaporate the organic solvent. The suspended NPs were centrifuged three times in 15 minutes cycles at the speed of 13 500 rpm using (Hermle Z 326 K, Germany) and washed with distilled water to remove the excess surfactant. NPs were collected and frozen in ultralow freezer at -80 °C for 24 h. The suspended NPs were freeze dried for 30 h at -50 °C using (Christ Alpha plus 1-4, Germany) freeze dryer. Figure 3.1 represents nanoprecipitation technique employed.

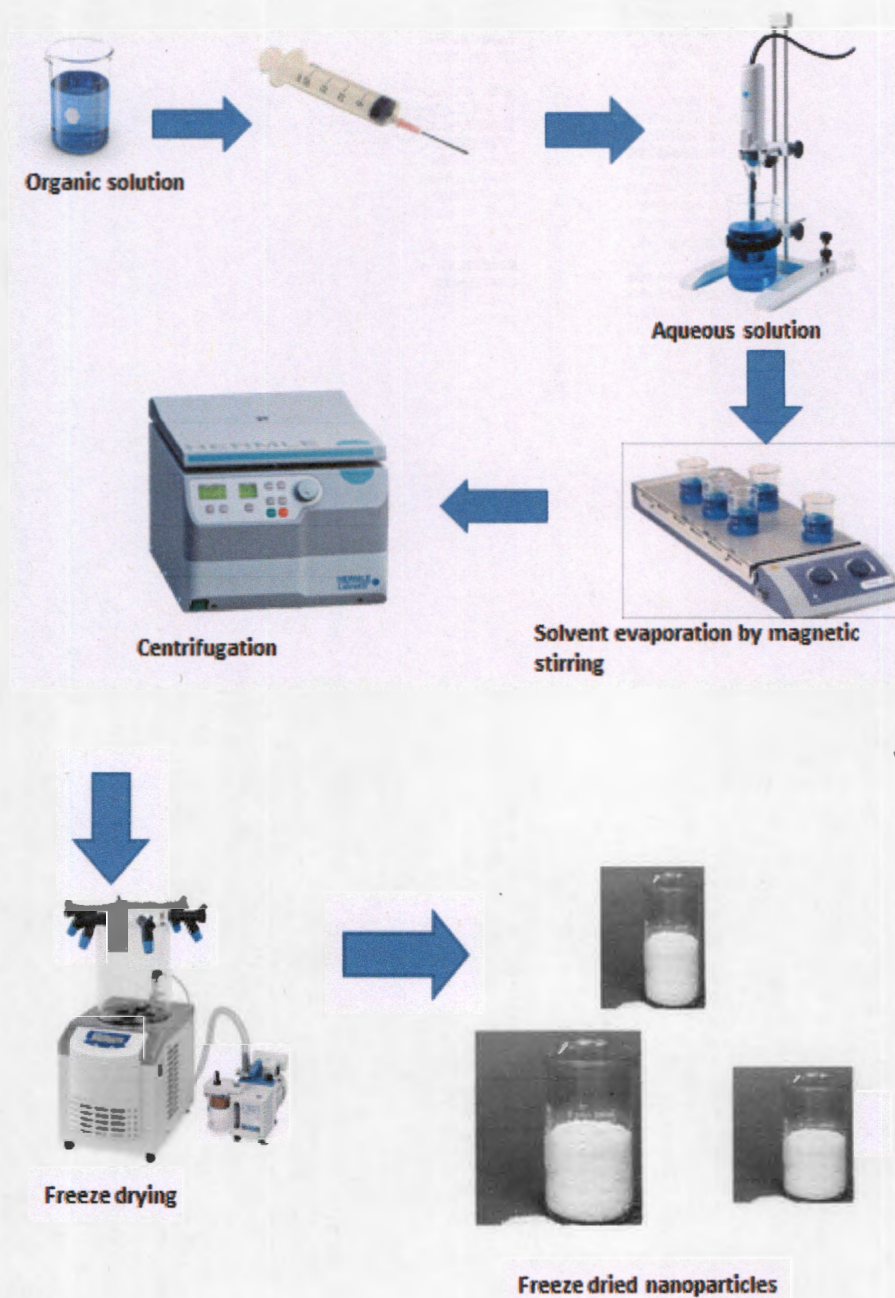


**Figure 3.1:** Schematic representation of nanoprecipitation method used for formation of NPs

### **3.8 Evaluation and characterization of Eud-RBV NPs**

#### **3.8.1 Particle size, PDI and zeta potential**

The freeze dried NPs were suspended in distilled water and transferred into clear cell and analysed by (Malvern Zetasizer nano ZS, UK) installed with DTS software. For average particle size measurement, the instrument applied dynamic light scattering (DLS) principle. It uses the intensity, volume, and number distribution in calculating average size and PDI. The software collects and interprets data for the particle size and zeta potential. Then mean particle diameter, and PDI were measured. The ZP was also measured from the same instrument by observing the oscillations in signal that result from light scattered by particles located in an electric field. All the parameters were measured three times at 25 °C and three repetitions were done. The two optimised NPs were labelled Eud-RBV(PVA) and Eud-RBV(POLO) NPs, and were chosen for further characterisation.

#### **3.8.2 Morphology study of Eud-RBV(PVA) NPs and Eud-RBV(POLO) NPs**

The two optimised Eud-RBV NPs were taken for morphological study through scanning electron microscope (FEI Quanta 250 FEG SEM, UK) operating at 10 kV. Samples were mounted on 12 mm aluminium specimen stubs with double sided carbon tape, coated with gold palladium and examined.

#### **3.8.3 Drug-excipients interaction determination by FTIR**

RBV, PVA, POLO, Eud, Eud-RBV(PVA) and Eud-RBV(POLO), were all scanned and recorded using (Varian 300 FTIR, US). The solid samples were placed on sample holder and analysed over a wavelength of 4000-400  $\text{cm}^{-1}$  using FTIR instrument.

### 3.8.4 Crystallinity study of Eud-RBV NPs through XRD

The nanoparticle crystal structure was analysed by x-ray power diffraction. The sample was placed in cold nitrogen at a temperature of 25 °C and centred in the beam of the X-ray. The evaluation of the crystal and collection of data were conducted using (Bruker APEXII CCD DUO diffractometer, Japan) which uses MoKa ( $k = 0.71073 \text{ \AA}^\circ$ ) radiation.

### 3.8.5 Encapsulation Efficiency determination

The amount of drug encapsulated within the polymer in NPs was determined by UV-vis spectrophotometry. The prepared samples were centrifuged three times at 13500 rpm for 15 min per cycle. The supernatant from the first cycle was taken and measured the absorbance using (Spectroquant Prove 300, Germany) UV-vis. The determined wavelength of RBV was 206 nm.

The encapsulation efficiency (EE) of the drug was calculated by the equation

$$EE = \frac{\text{initial drug amount} - \text{drug in the supernatant}}{\text{initial drug amount}} \times 100\%$$

### 3.8.6 *In vitro* drug release analysis

Accurately weighed 4 mg of each product (Eud-RBV(PVA), RBV and Eud-RBV(POLO)) in 3 triplicates and suspended in 4 mL of different buffer solutions i.e. PBS at pH 7.4, SIF at pH 4.6 and SGF at pH 1.2 separately in 5 mL Eppendorf tubes. The samples were then left in shaking water bath at 37 °C with constant shaking of 50 rpm. The 2 ml of samples were then taken out at a definite time interval from 0-6 h and replaced with a fresh medium. The sample taken was diluted to 10 ml with distilled water and monitored by using UV-vis spectrophotometer at wavelength 206 nm and this procedure was repeated two times. The measured absorbance was used to determine the corresponding concentration from the calibration curve.



### 3.8.7 Thermal analysis of Eud-RBV NPs

Thermogravimetric analysis and differential scanning calorimetry were performed using (TGA/DSC Spin Mettler, Germany). Samples pure RBV, Eud, Eud-RBV(PVA) and Eud-RBV(POLO) were weighted at different weights from 3.5-10.75 mg into aluminium pans. The nitrogen gas was used at the flow rate of 30 mL/min and the analysis done at a temperature range from 25 to 300 °C at heat rate of 10 °C /min. NPs were subjected to thermogravimetric analysis to investigate their thermal stability against the pure polymer and to assess their residual moisture content.

### 3.8.8 *In vivo* cytotoxicity study of Eud-RBV NPs

Preliminary *in vivo* toxicity testing was completed using *Daphnia magna*, a standard international species. Stock cultures were kept in 2.5 L tanks in *Daphnia* media which were replaced three times per week and kept at a temperature of 20 °C. *Daphnia* adults were fed on 5 mL of *Raphidocelis subcapitata* (microalgae) after each water change which occurred three times per week. Prior to the toxicity test adults were transferred to clean medium and neonates less than 24 hours old were collected for testing. All four constituents were tested, however for RBV and Eud only range finding (1 mg/L and 10 mg/L) concentrations were tested (Botha 2016). The *in vivo* study was done once.

The Eud-RBV(PVA) NPs and Eud-RBV(POLO) NPs had a full range tested. The acute immobilization test (OECD 202) was used for toxicity testing. Twenty-one neonates were used per concentration; tests were carried out in triplicate with each of the three 50mL beakers per concentration containing seven organisms. A 16 h light and 8 h dark cycle was applied for the duration of the test and the temperature was maintained at  $20 \pm 2^{\circ}\text{C}$  using a temperature controlled environmental room. At 24 h intervals the number of immobilized *Daphnia*, that is, any animal that was immobilized for more than 15 seconds, was counted. Any abnormal behaviour was also noted. The test was concluded after 48 h and analysis was performed using ToxRat solutions GmbH which is able to calculate and  $\text{LC}_x$  value using probit analysis.



## CHAPTER 4

### RESULTS AND DISCUSSION

#### 4.1 Calibration curve of RBV

Scanning of RBV was done in two different media namely, PBS at pH 7.4 and distilled water. The results showed absorbance maximum at 206 nm. The value corresponds to the reported value of approximately 207 nm (Kumar, 2013). The absorbance maxima graphs of RBV were similar in both media (Figure 4.1). The absorbance maxima were determined at different concentrations of RBV from 0-35ppm. An increase in absorbance with increase in RBV concentration was observed. On the basis of the results obtained from spectroscopic scanning, all the analytical data were analysed at 206 nm for drug content study, and for *in vitro* drug release study

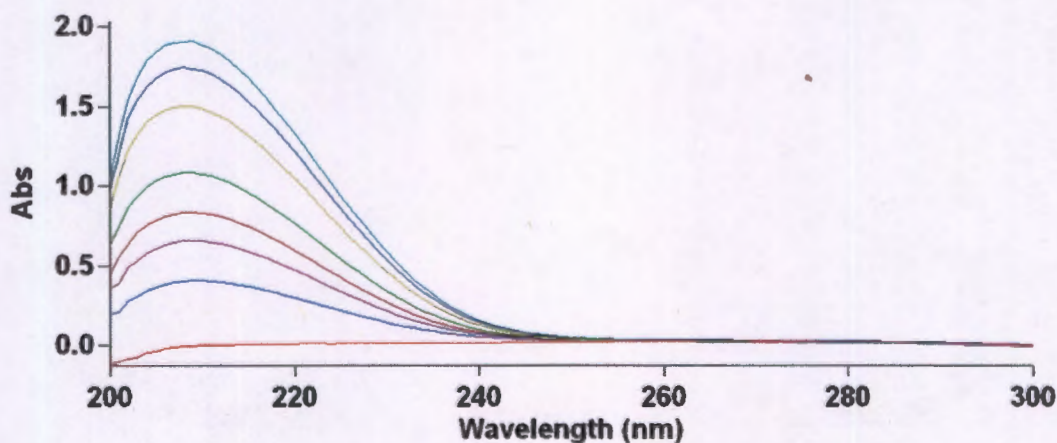


**Figure 4.1:** Absorbance maxima of RBV in PBS at pH 7.4

The calibration curve of RBV (Figure 4.2) was prepared by serial dilutions with PBS. It was then determined by plotting the absorbance as a function of the RBV concentration at 206nm.

The regression coefficient was 0.9855 and indicated a good linearity. Three trials were conducted in scanning of the drug in order to obtain the reproducible results. The measured absorbance was too close in all three trials. This gives a good average absorbance.

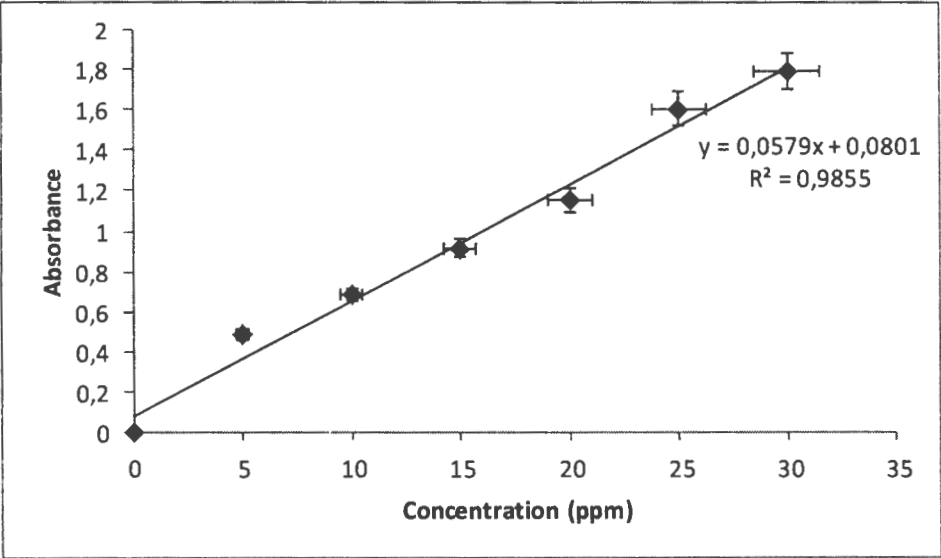


**Figure 4.2:** Calibration curve of RBV in PBS.

Calibration curve showed a minor deviation that indicated favourable accuracy of the adopted analytical methods. In the developed calibration curve, the value of  $R^2$  was obtained and indicated the accuracy of estimation regarding the drug content, EE and *in vitro* drug release in this research work (Zhang *et al.*, 2002).

#### 4.2 Average particle size analysis of Eud-RBV NPs

Nanoparticle size is a very useful parameter in nanotechnology and drug delivery systems. The NPs uptake and distribution within the human body depend on the size (Giannitrapani *et al.*, 2014b). The smaller NPs with diameter < 250 nm show quick absorption into bloodstream and are usually not taken into RES. The bigger NPs with a mean diameter > 400 nm are quickly captured by the RES and quickly cleared from the body by microphages. The literature suggests that, the smaller NPs ranging from 20-200 nm can be used for intravenous administration (Alexis *et al.*, 2008).



#### 4.2.1 Effect of organic solvent in average particle size of NPs

The average particle size of NPs prepared from acetone, EA and EtOH solvents were varied due to the differences in polarity and water-solvent interactions. It is proposed that the diffusion process might be altered, thus inducing changes in the average size (Bilati *et al.*, 2005). The profiles of the NPs average size obtained shown to increase in the order from EtOH, EA to acetone (Figure 4.3) and this follow the solubility trend of these solvents. A first requirement of mutual solubility is that the solubility parameter of the solute and that of the solvent should not differ too much (Galindo-Rodriguez *et al.*, 2004).

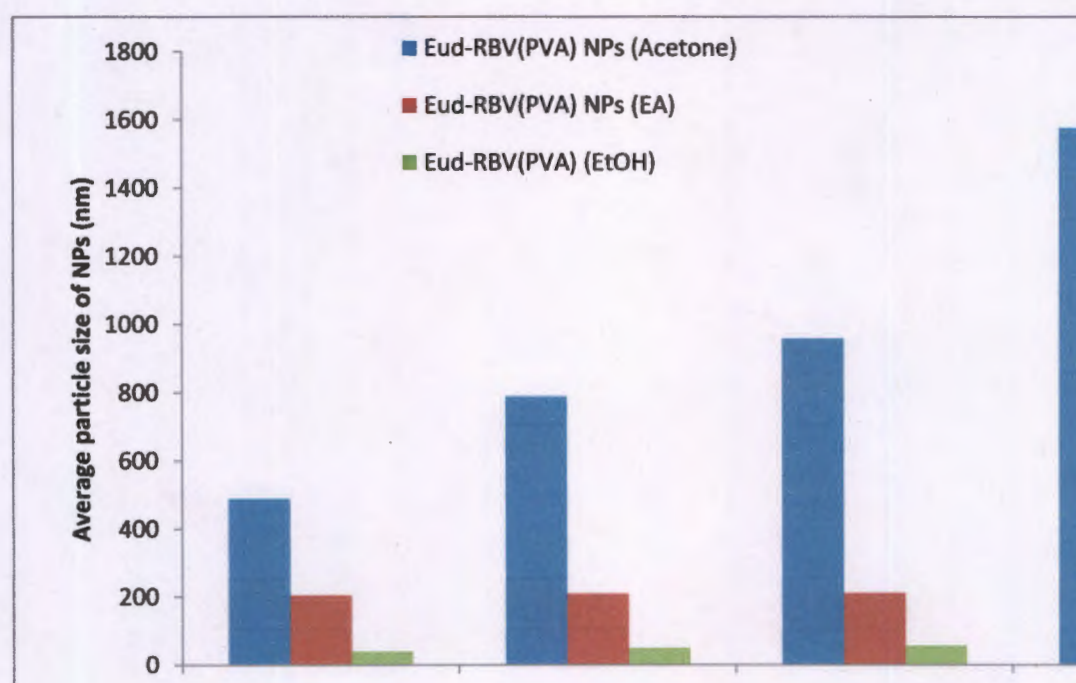


**Figure: 4.3:** Average particle size of NPs prepared varying PVA concentrations in EA and EtOH

The smaller the differences between solute and solvent, the higher the affinity and smaller the NPs size formed. In addition from the literature, the solvent-water values increase in order from alcohol < ketone < ester. Comparing at the same polymer concentration, the mean size of NPs formed from these solvents increases in the same order (Galindo-Rodriguez *et al.*, 2004). EtOH showing smallest solvent-water value produced the smallest NPs ranging from 24.4-88.1 nm. EA with moderate solvent-water value, gave middle values of 204.3-227.6 nm

and lastly acetone with the high solvent-water value gave the larger size of 489.2-1577.0 nm. The observed trend was similar in NPs formed when POLO was used as a surfactant. This approach suggests that the higher the solvent-water affinity the smaller the NPs formed.

The obtained results showed the average particle size ranging from 200-250 nm in all NPs when EA was used as an organic solvent. Therefore these results promise a good absorption and distribution in blood from oral administration as suggested by Alexis *et al* 2008. Moreover these results have met the minimum requirements for oral delivery as compared to the work done by (Hashim *et al.*, 2010; Kumar, 2013). NPs prepared using EA are further analysed and discussed in this work because their size is ideal for oral administration. It is thought that these NPs will have a low uptake into RES (Redhead *et al.*, 2001). The NPs formed from EtOH showed size ranging from 24.47-88.12 nm, therefore they were not further characterized since their size is ideal for intravenous but not oral administration.

#### **4.2.1 Effect of surfactant on NPs size analysis**

Surfactants are used to stabilise the NPs in aqueous solution in order to prevent aggregation or precipitation of water insoluble polymer (Akagi *et al.*, 2012). In this study there was a clear trend observed in size of NPs prepared from PVA and POLO, when EA was used. NPs prepared using PVA as surfactant tend to increase in average size (Figure 4.4) with the increase in PVA concentration; this trend was observed in all NPs prepared from three organic solvents. In general, this is because of the supersaturation effect of PVA and when organic solvent diffuses, it leads into larger size (Overhoff *et al.*, 2008).

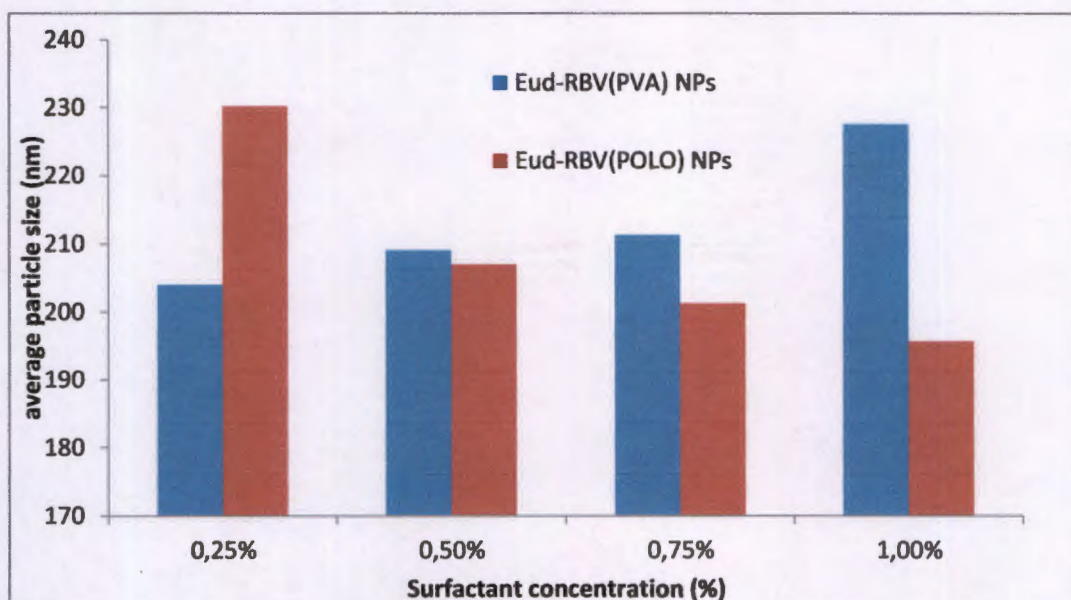


**Figure 4.4:** Effect of average particle size in various surfactant concentrations using EA

The observed behaviour was found in all the solvent. NPs prepared using POLO as surfactant decrease in size when the concentration increases. It has been documented that, surfactants such as POLO reduce the average particle size when the concentration increases, because of ability of POLO to reduce the surface tension of water, therefore polymer can also disperse more in aqueous medium (Dunn *et al.*, 1997).

#### 4.3 Effect of PDI on average particle size

PDI measures the particle size distribution of NPs and is obtained from photocorrelation spectroscopic analysis. It is a dimensionless number extrapolated from the autocorrelation function and ranges from a value 0.010 for monodisperse system and up to 0.500-0.700. Samples with very broad size distribution are characterized by high PDI values greater than 0.7 (Nidhin *et al.*, 2008). PDI is an important parameter in the performance of the NPs, as batches with wide particle distribution show significant variations in drug loading, drug release, bioavailability and efficacy (Kharia *et al.*, 2012). The obtained results showed a very low PDI values in NPs prepared from EA with the range from 0.012-0.149. Figure 4.5 and



4.6 show the percentage intensity against average size, as this determined the PDI. The NPs of EtOH show a PDI range of 0.045-0.427. All these results indicate the monodisperse system.

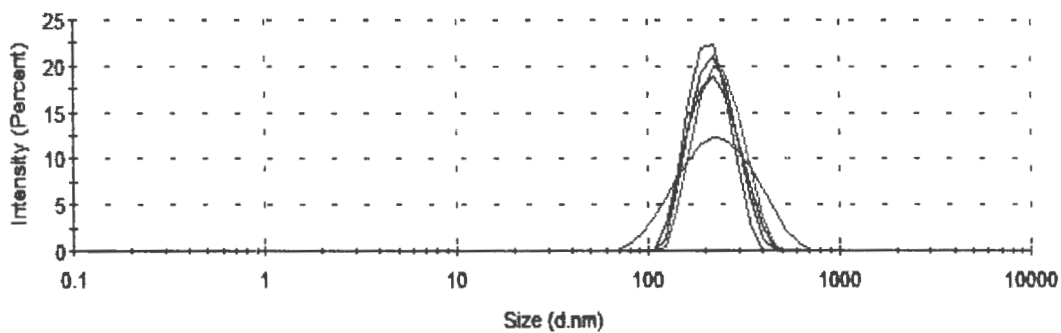


**Figure 4.5:** Intensity versus average size of all NPs prepared from PVA and EA

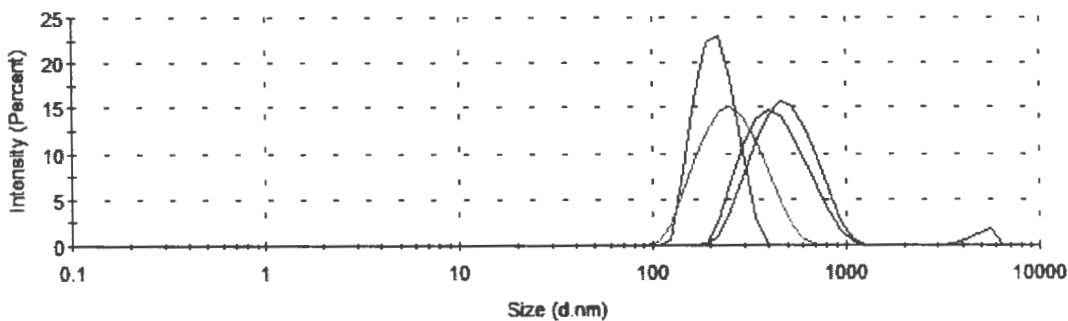


**Figure 4.6:** Intensity versus average size of all NPs prepared from POLO and EA

There was no observed trend in differences of PDI values of NPs in both surfactants. In general the PDI values of ethyl acetate NPs were lower than those of ethanol, in both surfactants.

#### 4.4. Effect of surfactant on Zeta Potential of NPs

Zeta potential (ZP) is a measure of the charge on the surface of the particle, as such the larger the absolute value of ZP, the greater the amount of charge (Hans & Lowman, 2002). ZP was

determined by Zetasizer ZS (Malvern instrument, UK). The dispersant used was water with a given dispersant dielectric constant and operating temperature was 25 °C. ZP values above 30 mV (positive or negative) lead to more stable NPs, because the repulsion between the particles is high and prevent the aggregation (Kharia *et al.*, 2012). From the obtained results, ZP values were higher in NPs of EA (Table 4.1), ranging from -24.0 to -57.0 mV. The NPs prepared from of PVA and EA measured ZP values greater than -50 mV, this indicates that the NPs were very stable in suspended condition and this reduces aggregation. This higher stability indicates that the suspended NPs can be stored in liquid medium (Abdelwahed *et al.*, 2006). Whereas NPs prepared from POLO measured the ZP of -24.0 to -38.0 mV, those NPs with ZP values less than -30 mV were not stable enough. The samples were then left lyophilized so that they can last longer without changing their properties and be used for further stability studies such as TGA and DSC.

**Table 4.1:** Variation of ZP in NPs prepared using EA

NPs prepared using PVA surfactant	ZP	NPs prepared using POLO surfactant	ZP
0.25% PVA	-54.4	0.25% POLO	-38.3
0.50% PVA	-53.3	0.50% POLO	-29.3
0.75% PVA	-57.0	0.75% POL	-25.4
1.0% PVA	-55.3	1.0% POLO	-24.0

The data obtained from EtOH as solvent show a lower ZP values (Table 4.2) as compared to their EA counterparts. In this case, all the PVA NPs measured ZP greater than -22 mV, suggests the medium stability. The POLO NPs were all less than -20 mV, therefore from the data, it is evident that all the POLO in EtOH NPs were unstable in a suspended condition.



**Table 4.2:** Variation of ZP values of NPs prepared using EtOH

<b>NPs prepared using PVA surfactant</b>	<b>ZP</b>	<b>NPs prepared using POLO surfactant</b>	<b>ZP</b>
0.25% PVA	-35.7	0.25% POLO	-18.5
0.50% PVA	-22.3	0.50% POLO	-14.2
0.75% PVA	-31.7	0.75% POLO	-6.88
1.0% PVA	-22.6	1.0% POLO	-5.47

The literature suggests that, it is because polymers such as Eud impart a negative charge to the surface, whereas non-ionic surfactant such as POLO turns to reduce the absolute value of the ZP (Kumar, 2013). This suggests that the particles should not be stored in a liquid suspension form but rather they should be stored in a lyophilized state (Abdelwahed *et al.*, 2006). Immediately before the administration, they should be reconstituted, as such type of NPs stored in colloidal stage have more stability problem than those stored in the dry form (Abdelwahed *et al.*, 2006).

## 4.5 Selection of optimised NPs

In the development of agents with anti-haemolysis effects, the surface properties and uptake pathways of erythrocytes/red blood cells (RBC) should be taken into consideration (Guo *et al.*, 2015). The surface of erythrocytes is negatively charged and 90 % of the net charge comes from sialic acid on the glycoprotein and glycolipids on the RBC surface (Guo *et al.*, 2015). Positively charged particles and molecules have been shown to interact with the interior of the bilayer, result into binding and penetration (Verma & Stellacci, 2010). Therefore, a negative charge on the particle surface might reduce the association with RBC.

The selection of optimised NPs was based on the results obtained from zetasizer such as size, PDI and ZP. These three physicochemical properties determine the performance of the NPs (He, 2010). The two chosen NPs have the average particle size between 200-250 nm, with low PDI of 0.012-0.149 and high ZP of over -29.0 mv. These NPs were both prepared from EA and 0.50% PVA or 0.50% POLO (Table 4.1). Therefore the further characterisation will be done on these NPs, whereby 0.50% PVA will be named 'Eud-RBV(PVA) NPs and 0.50% POLO will be 'Eud-RBV(POLO) NPs.

### 4.5.1 FTIR analysis

FTIR was used to determine the drug excipients interaction within the formulated NPs. The FTIR of the pure RBV, Eud and Eud-RBV NPs were recorded and compared. The spectrum of Eud (Figure 4.7) was characterized by one band at  $1705\text{ cm}^{-1}$  that is assigned to the C=O vibration of the carboxylic acid group and OH stretch at  $3000\text{ cm}^{-1}$  (Kumar, 2013). For bands at  $1480$  and  $1447\text{ cm}^{-1}$  which can be assigned to  $\text{CH}_2$  and  $\text{CH}_3$  bending corresponding a minor variation in the ratio of the copolymer

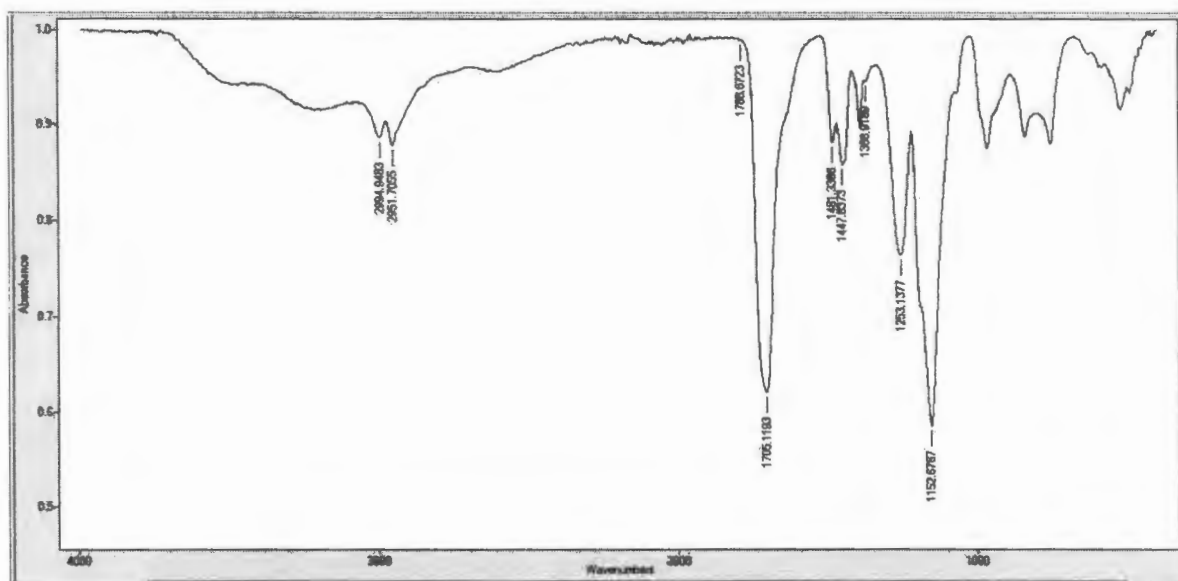


**Figure 4.7:** Eud FTIR spectrum

RBV scan showed a peak at  $3448.25\text{ cm}^{-1}$  that indicates moderate N-H stretch for primary amine (Figure 4.8). Peaks at  $3245.51$  and  $3341.9\text{ cm}^{-1}$  for strong O-H stretches of free alcohols. Peak  $1486.96$  for aromatic ring.  $1655$  for strong C=O stretch whereas  $1484$  and  $1437.47\text{ cm}^{-1}$  stand for moderate C-C bonds on the ring.

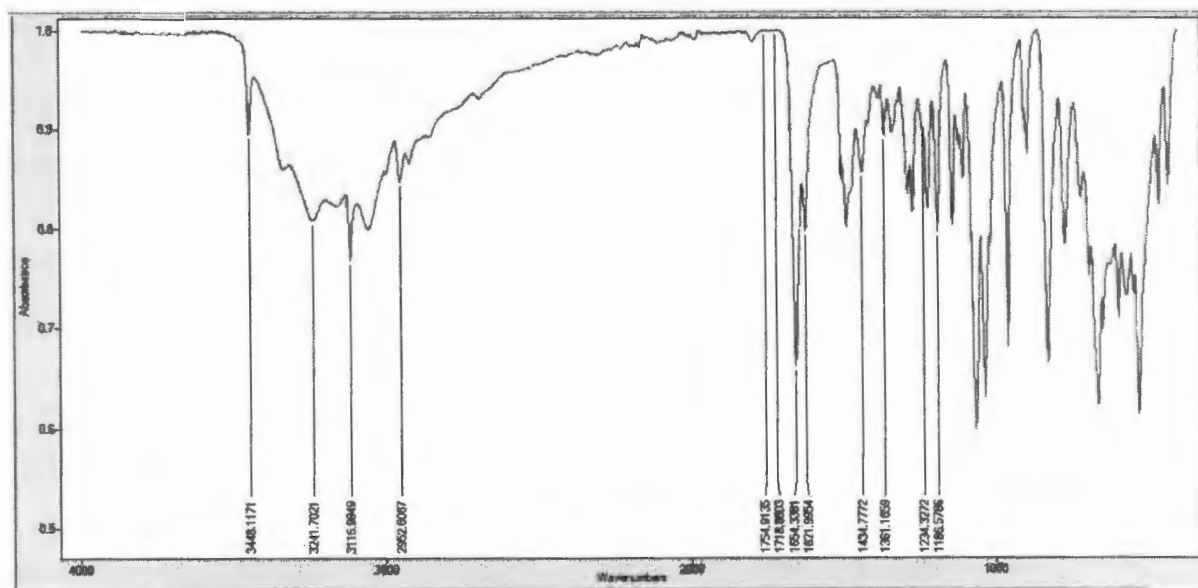


**Figure 4.8:** RBV FTIR spectrum

All the major peaks related to hydroxyl and acetate groups were observed. The larger bands observed between 3600 and 3200  $\text{cm}^{-1}$  are linked to the stretching O-H from the intermolecular and intramolecular hydrogen bonds (Figure 4.9 and 4.10). The vibrational band observed between 2840 and 3000  $\text{cm}^{-1}$  refers to the stretching C-H from alkyl group and the peaks between 1750 and 1600  $\text{cm}^{-1}$  are due to the stretching C=O and C-O from acetate group. This suggests that Eud formed the outer membrane of the nanoparticle. The appearance of the drug peaks may indicate that some drug is adsorbed on the polymer surface (Zhu *et al.*, 2015). The FTIR spectra of both prepared NPs were the same, regardless of surfactant and solvent used.

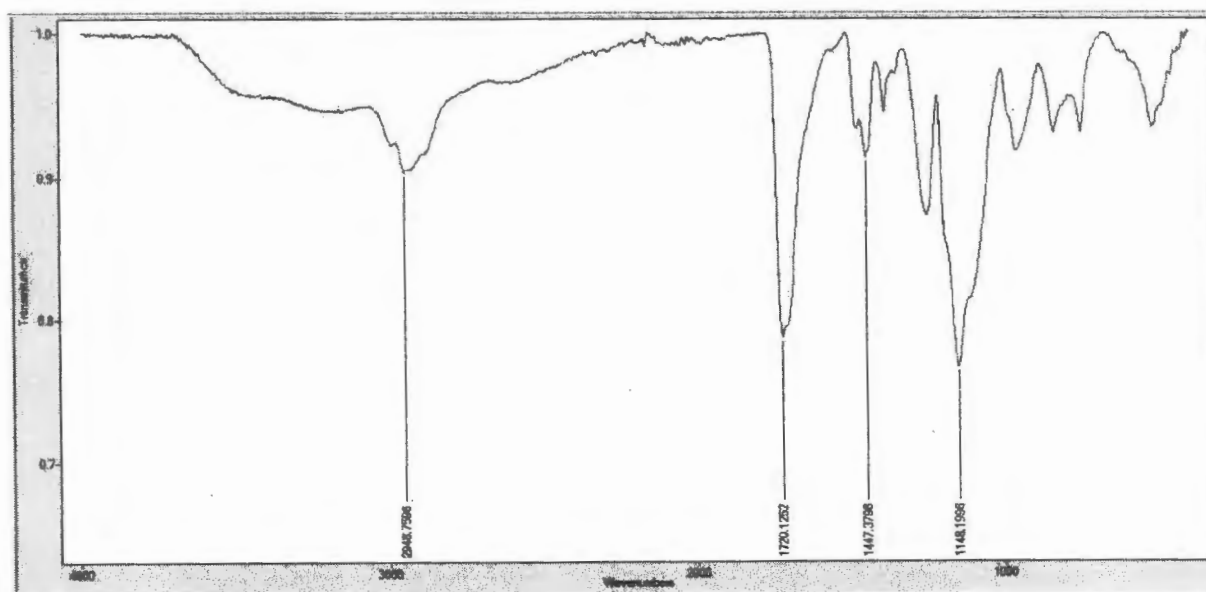


**Figure 4.9** FTIR spectrum for Eud-RBV(PVA) NPs

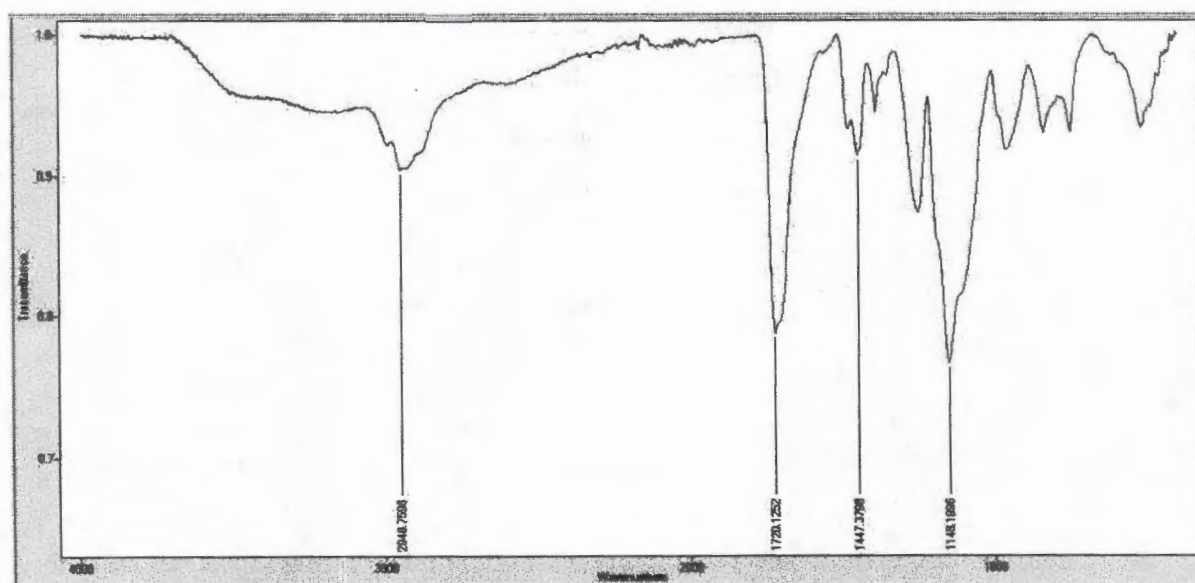


**Figure 4.10:** FTIR spectrum for Eud-RBV(POLO) NPs

4.5.2 XRD analysis

Powder X-ray diffraction study is usually used to evaluate both polymer-drug interactions and the state of a drug in a polymer mixture (Liu *et al.*, 2004). The crystal form of the NPs was carried out by XRD. The RBV showed characteristics crystalline sharp peaks (Fig 4.6), whereas Eud showed peaks of moderately low intensity and broader representing the amorphous form of the polymer (Fig 4.6). The two NPs consist of broad peak of the polymer and hence they are amorphous.

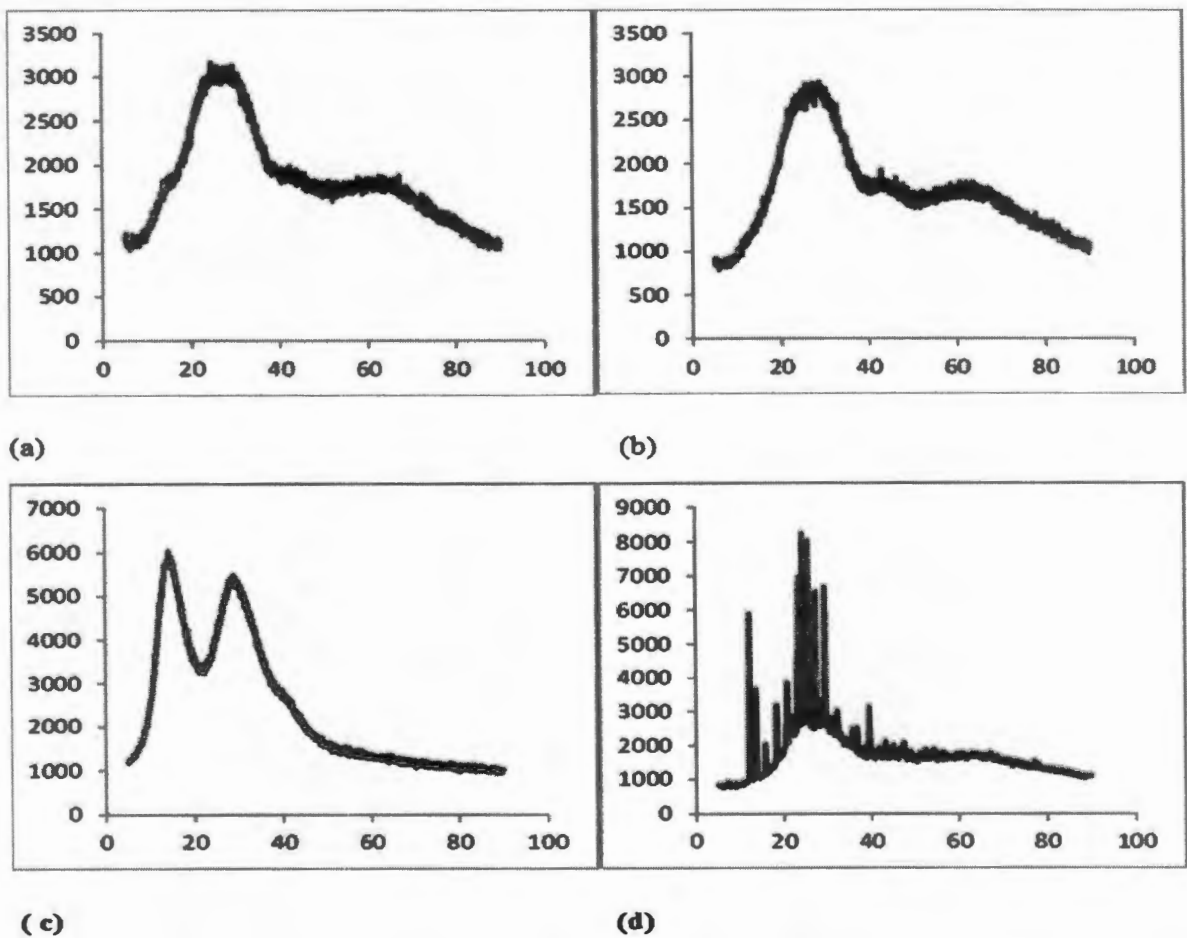
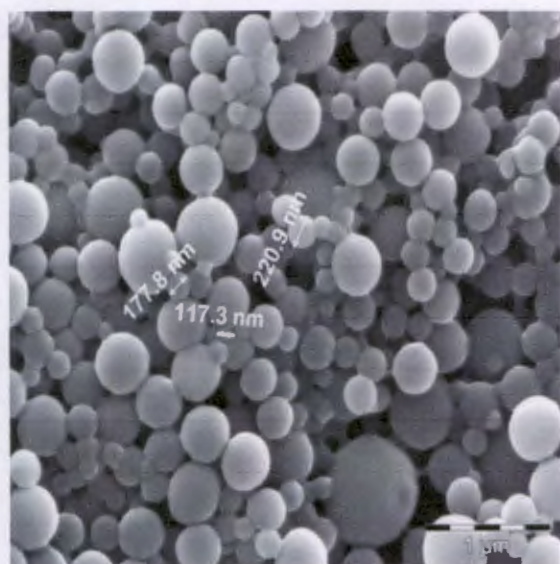


**Figure 4.11:** XRD results where y axis represents counts per second and x axis is theta degree; (a) Eud-RBV(PVA) NPs , (b) Eud-RBV(POLO) NPs, (c) pure Eud (d) pure RBV

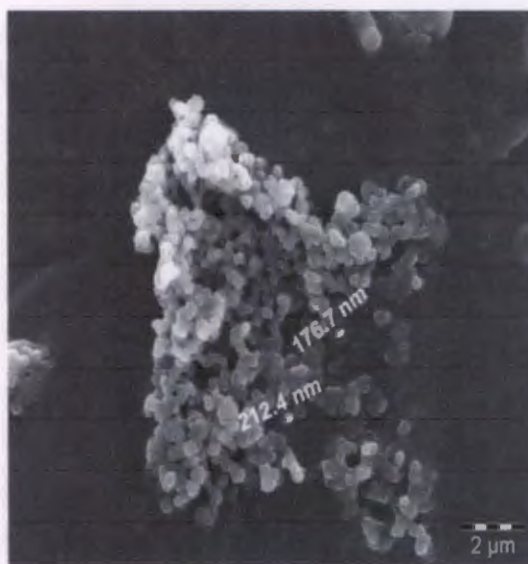


### 4.5.3 Morphology of Eud-RBV NPs through SEM

Two optimised NPs, namely, Eud-RBV(PVA) NPs and Eud-RBV(POLO) NPs that showed good particle size, PDI and ZP were taken for morphological study using SEM. These NPs were prepared from the same organic solvents and different surfactants. The figure 4.5.a. shows the SEM image of smooth and spherical NPs prepared using PVA and Figure 4.5.b depicts the SEM photographs of formulation prepared from 0.50% POLO which shows that particles were also spherical, and being joined in close association.



(a)



(b)

**Figure 4.12:** SEM images (a) Eud-RBV(PVA)NPs and (b) Eud-RBV(POLO) NPs

### 4.5.4 Encapsulation Efficiency

EE is a significant parameter that defines the concentration of the incorporated drug detected in the NPs over the initial concentration used to make the NPs (Ammar, 1997). From the results obtained, both optimised NPs measured EE greater than 96 %, indicating that the larger amount of drug has been trapped in NPs, however RBV exhibits hydrophilic nature then the drug could also be surface adsorbed. Bilati, 2005 used nanoprecipitation technique to for entrapment of hydrophilic drugs, and he obtained high EE of more than 75%. The

results show a good target drug delivery and thus findings made by (Bilati, 2005).The solvents used and surfactant types and concentrations did not have an effect on encapsulation.

4.5.5 Drug release studies

The release properties of polymeric NPs are one of the most essential features in polymer-drug NPs because of the proposed application in sustained drug delivery systems (Hans & Lowman, 2002). The release mechanism of the polymer depends on its rate of dissolution. The slower the rate the slower the release and hence the prolonged drug circulation within the blood stream.

The *in vitro* drug release was performed to investigate the polymer’s ability to release the drug after oral administration. The simulated buffers were prepared with the same GIT conditions. The results showed the initial fast release of the drug (Figure 4.13). It is suggested that some drug was localized on the surface of the nanoparticles. This fast release could also result from the amorphous nature of the NPs observed from XRD analysis. Both Eud-RBV NPs displayed the similar release behaviour. The pure drug was quickly released, due to its hydrophilic nature. The drug release in PBS was the same as in SIF.

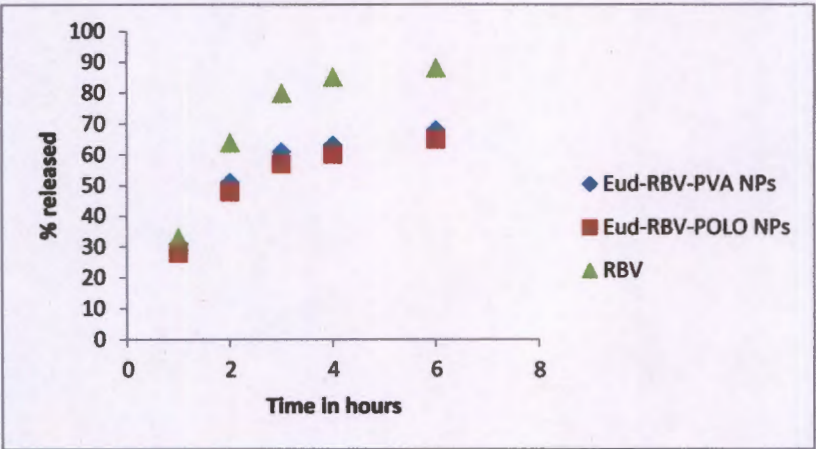


**Figure 4.13:** Drug release profile of Eud-RBV(PVA) NPs, Eud-RBV(POLO) NPs and RBV in SIF



The Eud is an enteric pH-dependent copolymer and is soluble above pH 5.5 medium, so all the buffers prepared were pH controlled. The other parameter may be due to the hydrophilicity of RBV, therefore once release it dissolves quicker.

### 4.5.6 Thermal analysis

Thermal analysis is commonly used in the drug delivery field to obtain information about drug-polymer interactions and formulation effects on these interactions (Silva-Junior et al., 2008; Gaisford & Buckton, 2001). The thermal properties of RBV, Eud and two of drug-loaded polymeric nanoparticles (Eud-RBV(PVA) NPs and Eud-RBV(POLO) NPs) were determined using TGA and DSC. From Table 4.3, it is observed that the pure drug is not thermal stable on its own but with the encapsulation of the polymer with the drug, it shows more stable nanoparticles with less percentage weight loss after 30 minutes.

**Table 4.3:** TGA results for RBV, Eud, Eud-RBV(PVA) NPs and Eud-RBV(POLO) NPs

Sample	Initial weight(mg)	Weight loss (mg)	% weight loss
Eud-RBV(PVA) NPs	3.100	0.7091	22.8748
Eud-RBV(POLO) NPs	4.500	0.8065	17.9218
RBV	10.75	5.7793	53.7605
Eud	10.12	0.9831	9.7144

The results also confirmed the trend observed from the Zeta potential results. The NPs showed a lower thermal stability as compared to the pure polymer. The results also agreed with the work done by (Fitzgerald & Corrigan, 1996), Venier-Juleinne & Benoit, 1996 & Mu & Feng, 2002).

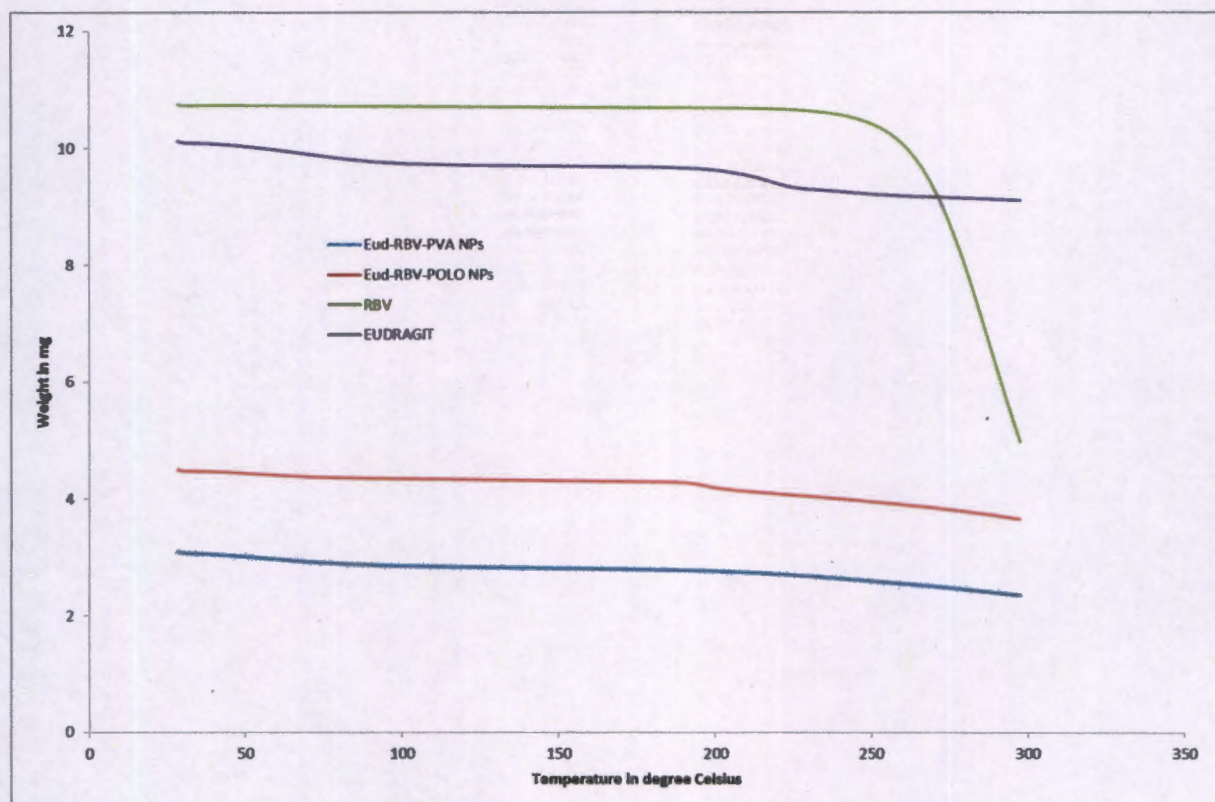


**Figure 4.14:** TGA Curves of RBV, Eud-RBV(PVA) NPs, Eud-RBV(POLO) NPs and Eud



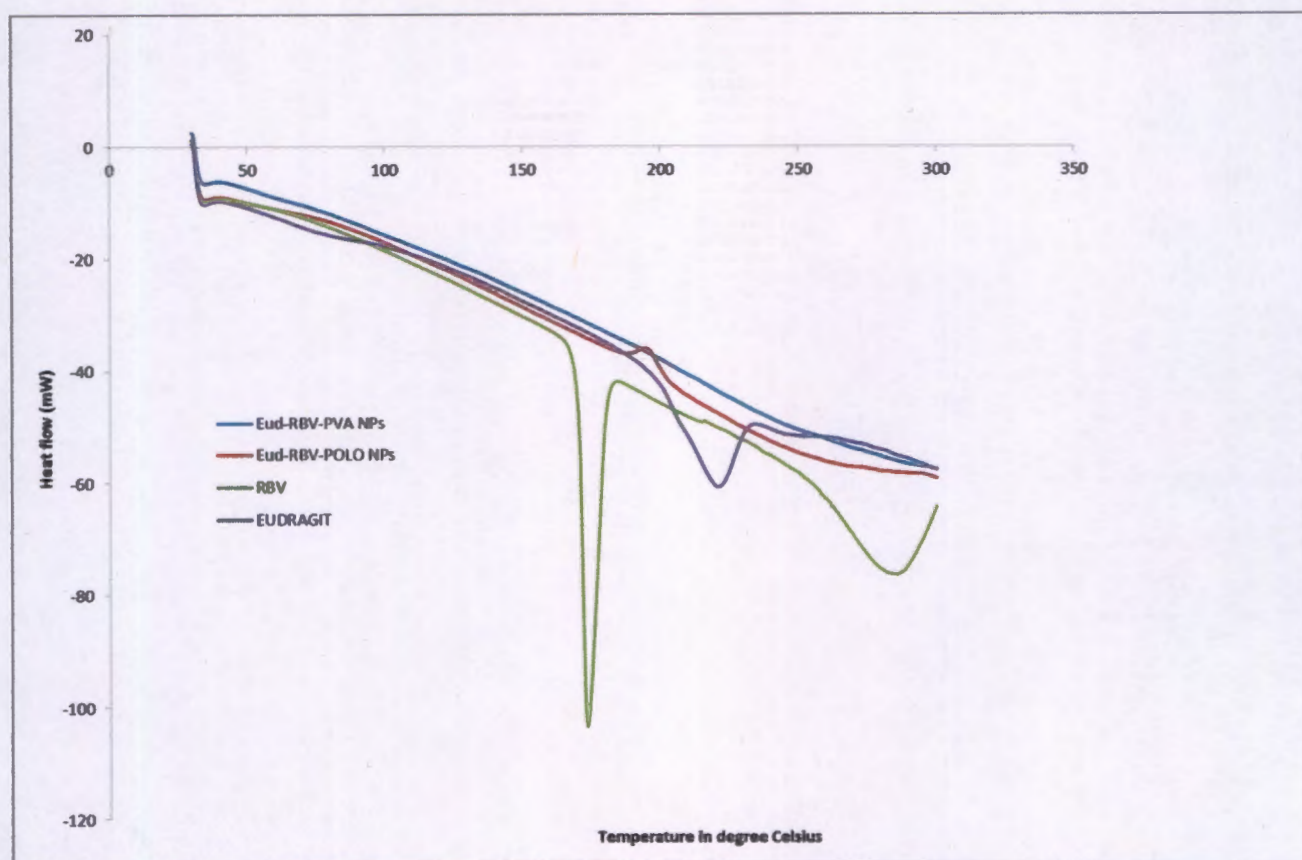


**Figure 4.15:** DSC Curves of RBV, Eud-RBV(PVA) NPS, Eud-RBV(POLO) NPS and Eud

From Table 4.3 and Figure 4.14 and 4.15 above it is observed that the pure drug is not stable on its own but with the encapsulation of the polymer with the drug, it shows more stable nanoparticles with less percentage weight loss. It could also be associated with the amorphous state of the nanoformulation as compared to the pure polymer

#### 4.5.7 *In vivo* cytotoxicity studies

The *in vivo* cytotoxicity is very important property since it tells whether a substance is toxic or compatible to living cells. In this study a *Daphnia magna* was used as living organisms and the optimised NPS were introduced. *Daphnia magna*, have been in use since 1960s as a standard species in acute and chronic aquatic toxicity testing (Botha, 2016).

The control group showed 100% survival throughout the study validating all tests conducted. The RBV range finding exhibited toxicity below 10% for both concentrations tested and

since the OECD tests guideline allows even the control to have a 10% mortality there was no toxicity observed. The Eud however showed 14.3% mortality at 1 mg/L and 28.6% mortality at 10 mg/L, a full range of testing needs to occur to determine an LC50 (Botha, 2016).

The Eud-RBV(PVA) NPs showed no toxicity after a period of 48h, while the Eud-RBV(POLO) NPs showed a lethal concentration where 10% of the organisms would be affected (LC<sub>10</sub>) of 23.07 mg/L within 24 h of exposure. Concentration effect curves (Figure14.16 and 14.7) show the concentration curve used for probit analysis. Changes in swimming and for aging behaviour was seen during exposures where nanomaterials formed mechanical interference.

**Table 4.4:** The results of the probit analysis showing LCx values for Eud-RBV(PVA)NPs and Eud-RBV(POLO)NPs.

Toxicity Metric	Eud-RBV(PVA) NPs		
	LC <sub>10</sub>	LC <sub>20</sub>	LC <sub>50</sub>
Value [mg/L]	n.d.	n.d.	n.d.
lower 95%-cl	n.d.	n.d.	n.d.
upper 95%-cl	n.d.	n.d.	n.d.
Toxicity Metric	Eud-RBV(POLO) NPs		
	LC <sub>10</sub>	LC <sub>20</sub>	LC <sub>50</sub>
Value [mg/L]	23.07	n.d.	n.d.
lower 95%-cl	n.d.	n.d.	n.d.
upper 95%-cl	n.d.	n.d.	n.d.



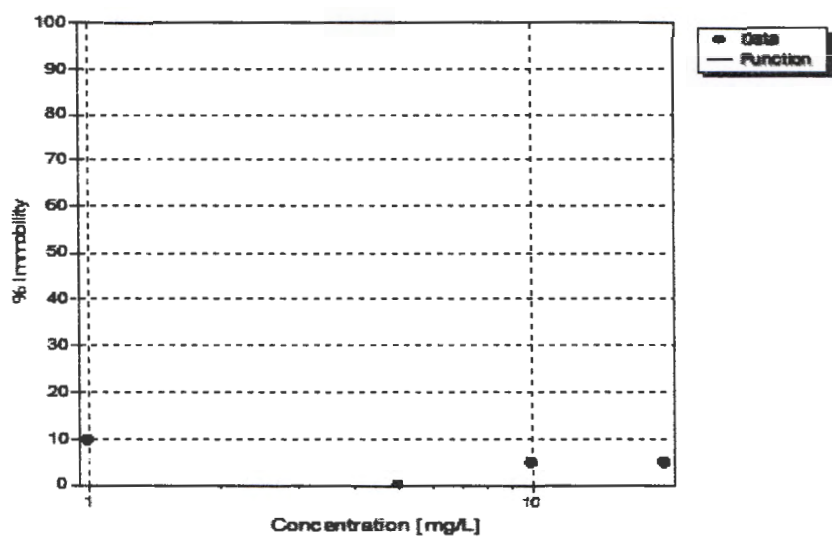


**Figure 4.16:** Concentration-effect curve showing the influence of the Eud-RBV(PVA) NPs on immobility of the introduced *Daphnia magna* as observed after 24 h

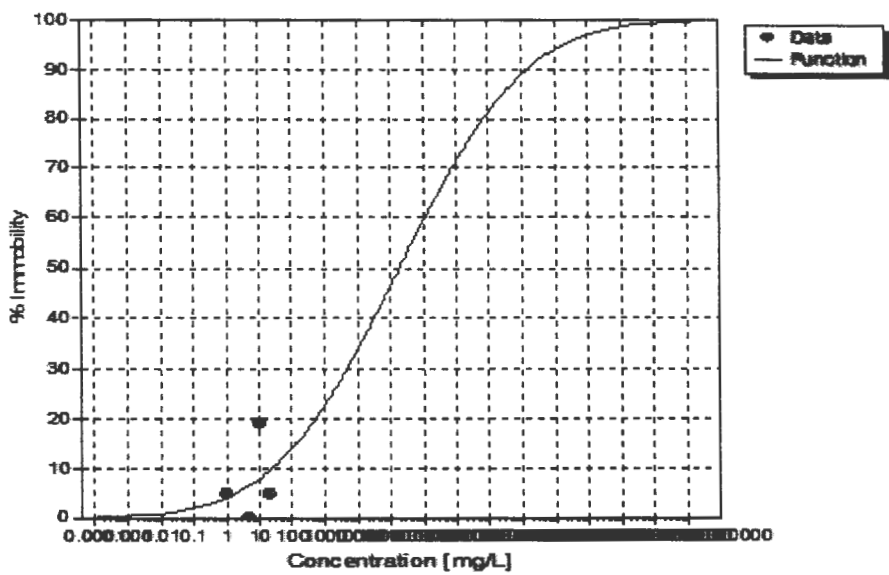


**Figure 4.17:** Concentration-effect curve showing the influence of the Eud-RBV(POLO) NPs on immobility of the introduced *Daphnia magna* as observed after 24 h

Low toxicity levels were seen for all nanomaterials and constituents tested within this study. Since predictions don't, at this point, envisage a concentration higher than 10 mg/L to be found within the environment the levels are within acceptable ranges. It is however necessary to do one higher concentration, perhaps 40mg/L in order to get conclusive results.

## CHAPTER 5

### CONCLUSIONS AND RECOMENDATIONS

#### 5.1 Conclusions

RBV was successfully encapsulated into Eud by nanoprecipitation technique. EA is preferred organic solvent for preparing Eud-RBV NPs ranging between 200-250 nm and PVA is also a preferred surfactant. The Optimised NPs results showed a good physiochemical properties thought out the characterisations. The high ZP that demonstrated a high stability of NPs liquid suspension and this data assists in the storage and life of the NPs (Abdelwahed, 2006). A spherical morphology was observed in both optimised the NPs. The FTIR confirmed the high EE by showing the major peaks of the drug in the NPs. This also imply that some drug amount was located on the surface of the polymer and in addition, the *in vitro* drug release studies showed a rapid drug release.

There are numerous studies done in attempt to improve the effectiveness of RBV though the application of nanotechnology. But the most important parameters such as size and ZP were not controlled. In his work, (Kumar, 2013) formulated PLGA-RBV NPs using double emulsion method. The results showed a low ZP of -6.51-13.8 mV and high PDI ranging from 0.45-0.94, with average size ranging between 342.0-635.5 nm. In another attempt, (Hashim *et al.*, 2010) used niosomes as the drug carrier for RBV, but the EE was very low between 4,89-14.4%. Therefore from the results obtained in this work, nanoprecipitation technique offers the best physiochemical properties and Eud L100 is preferred polymer for preparing RBV NPs. Furthermore the *in vivo* cytotoxicity showed a 100% survival in the Eud-RBV(PVA) NPs. Therefore the results in this study promise to improve the therapeutic effectiveness of RBV. In conclusion, this study has achieved the major objectives and the NPs formed may offer an alternative in the near future for the treatment of HCV and could potentially improve patient compliance.

#### 5.2 Recommendations

More *in vivo* studies are needed on swimming and foraging behaviour in *Daphnia* using higher concentration of more than 40 mg/L and this will confirm the results obtained using a lower concentration. *In vitro* studies using human cells will add more value to the *in vivo* results obtained. Furthermore, the physical mixture of Eud, RBV and surfactant will be assayed for possible confirmation that the incorporation of RBV in the NPs could actually change the drug thermal behaviour

## REFERENCES

- Abdelwahed, W., Degobert, G., Stainmesse, S. & Fessi, H. 2006. Freeze-drying of nanoparticles: formulation, process and storage considerations. *Advanced drug delivery reviews* (Vol. 58. pp. 1688-1713).
- Aguilar, L.E., Unnithan, A.R., Amarjargal, A., Tiwari, A.P., Hong, S.T., Park, C.H., et al. 2015. Electrospun polyurethane/Eudragit® L100-55 composite mats for the pH dependent release of paclitaxel on duodenal stent cover application. *International journal of pharmaceutics*, 478(1):1-8.
- Alexis, F., Pridgen, E., Molnar, L.K. & Farokhzad, O.C. 2008. Factors affecting the clearance and biodistribution of polymeric nanoparticles. *Molecular pharmaceutics*, 5(4):505-515.
- Angelova, N. & Hunkeler, D. 1999. Rationalizing the design of polymeric biomaterials. *Trends in biotechnology*, 17(10):409-421.
- Avgoustakis, K., Beletsi, A., Panagi, Z., Klepetsanis, P., Livanou, E., Evangelatos, G., et al. 2003. Effect of copolymer composition on the physicochemical characteristics, in vitro stability, and biodistribution of PLGA-mPEG nanoparticles. *International journal of pharmaceutics*, 259(1):115-127.
- Berak, H., Laskus, T., Kołakowska-Rządźka, A., Wasilewski, M., Stańczak, J.J., Bardadin, K., et al. 2014. Peginterferon alfa-2a and peginterferon alfa-2b combined with ribavirin in patients with genotype 1 chronic hepatitis C: results of a prospective single-centre study. *Advances in medical sciences*, 59(2):261-265.
- Bilati, U., Allémann, E. & Doelker, E. 2005. Development of a nanoprecipitation method intended for the entrapment of hydrophilic drugs into nanoparticles. *European journal of pharmaceutical sciences*, 24(1):67-75.

Botha, T.L., Boodhiab, K. & Wepenaar, V. 2016. Adsorption, uptake and distribution of gold nanoparticles in *Daphniamagna* following long term exposure. *Aquatic Toxicology*, 170 104–111

Brookes, S., Biessels, P., Ng, N.F., Woods, C., Bell, D.N. & Adamson, G. 2006. Synthesis and characterization of a hemoglobin-ribavirin conjugate for targeted drug delivery. *Bioconjugate chemistry*, 17(2):530-537.

Chakravarti, A., Ashraf, A. & Malik, S. 2013. A study of changing trends of prevalence and genotypic distribution of hepatitis C virus among high risk groups in North India. *Indian journal of medical microbiology*, 31(4):354.

Couvreux, P. & Vauthier, C. 2006. Nanotechnology: intelligent design to treat complex disease. *Pharmaceutical research*, 23(7):1417-1450.

Crotty, S., Cameron, C. & Andino, R. 2002. Ribavirin's antiviral mechanism of action: lethal mutagenesis? *Journal of molecular medicine*, 80(2):86-95.

Dong, S.D., Lin, C.-C. & Schroeder, M. 2013. Synthesis and evaluation of a new phosphorylated ribavirin prodrug. *Antiviral research*, 99(1):18-26.

Dubuisson, J. & Cosset, F.-L. 2014a. Virology and cell biology of the hepatitis C virus life cycle—An update. *Journal of hepatology*, 61(1):S3-S13.

Dubuisson, J. & Cosset, F.-L. 2014b. Virology and cell biology of the hepatitis C virus life cycle – An update. *Journal of Hepatology*, 61(1, Supplement):S3-S13.

Dubuisson, J., Helle, F. & Cocquerel, L. 2008. Early steps of the hepatitis C virus life cycle. *Cellular microbiology*, 10(4):821-827.

Dunn, S.E., Coombes, A.G., Garnett, M.C., Davis, S.S., Davies, M.C. & Illum, L. 1997. In vitro cell interaction and in vivo biodistribution of poly (lactide-co-glycolide) nanospheres surface modified by poloxamer and poloxamine copolymers. *Journal of controlled release*, 44(1):65-76.

Eloy, J.O., Claro de Souza, M., Petrilli, R., Barcellos, J.P.A., Lee, R.J. & Marchetti, J.M. 2014. Liposomes as carriers of hydrophilic small molecule drugs: Strategies to enhance encapsulation and delivery. *Colloids and Surfaces B: Biointerfaces*, 123:345-363.

Fitzgerald, J. & Corrigan, O. 1996. Investigation of the mechanisms governing the release of levamisole from poly-lactide-co-glycolide delivery systems. *Journal of controlled release*, 42(2):125-132.

Galindo-Rodriguez, S., Allémann, E., Fessi, H. & Doelker, E. 2004. Physicochemical parameters associated with nanoparticle formation in the salting-out, emulsification-diffusion, and nanoprecipitation methods. *Pharmaceutical research*, 21(8):1428-1439.

Gao, Y., Xie, J., Chen, H., Gu, S., Zhao, R., Shao, J., et al. 2014. Nanotechnology-based intelligent drug design for cancer metastasis treatment. *Biotechnology advances*, 32(4):761-777.

Giannitrapani, L., Soresi, M., Bondi, M.L., Montalto, G. & Cervello, M. 2014a. Nanotechnology applications for the therapy of liver fibrosis. *World J Gastroenterol*, 20(23):7242-7251.

Giannitrapani, L., Soresi, M., Bondi, M.L., Montalto, G. & Cervello, M. 2014b. Nanotechnology applications for the therapy of liver fibrosis. *World journal of gastroenterology: WJG*, 20(23):7242.

Guo, H., Sun, S., Yang, Z., Tang, X. & Wang, Y. 2015. Strategies for ribavirin prodrugs and delivery systems for reducing the side-effect hemolysis and enhancing their therapeutic effect. *Journal of controlled release*, 209:27-36.

Guterres, S.S., Alves, M.P. & Pohlmann, A.R. 2007. Polymeric Nanoparticles, Nanospheres and Nanocapsules, for Cutaneous Applications. *Drug Target Insights*, 2:147-157.

Hans, M. & Lowman, A. 2002. Biodegradable nanoparticles for drug delivery and targeting. *Current Opinion in Solid State and Materials Science*, 6(4):319-327.

- Hao, S., Wang, B., Wang, Y., Zhu, L., Wang, B. & Guo, T. 2013. Preparation of Eudragit L 100-55 enteric nanoparticles by a novel emulsion diffusion method. *Colloids and Surfaces B: Biointerfaces*, 108:127-133.
- Hashim, F., El-Ridy, M., Nasr, M. & Abdallah, Y. 2010. Preparation and characterization of niosomes containing ribavirin for liver targeting. *Drug delivery*, 17(5):282-287.
- Haznedar, S. & Dortunç, B. 2004. Preparation and in vitro evaluation of Eudragit microspheres containing acetazolamide. *International Journal of Pharmaceutics*, 269(1):131-140.
- Iwasaki, Y., Ikeda, H., Araki, Y., Osawa, T., Kita, K., Ando, M., et al. 2006. Limitation of combination therapy of interferon and ribavirin for older patients with chronic hepatitis C. *Hepatology*, 43(1):54-63.
- Jain, K.K. 2012. The handbook of nanomedicine: Springer Science & Business Media.
- Karoney, M.J. & Siika, A.M. 2013. Hepatitis C virus (HCV) infection in Africa: a review. *Pan African Medical Journal*, 14(1).
- Katara, R. & Majumdar, D.K. 2013. Eudragit RL 100-based nanoparticulate system of aceclofenac for ocular delivery. *Colloids and Surfaces B: Biointerfaces*, 103:455-462.
- Kharia, A., Singhai, A. & Verma, R. 2012. Formulation and evaluation of polymeric nanoparticles of an antiviral drug for gastroretention. *Int J Pharm Sci Nanotechnol*, 4:1557-1562.
- Kopeček, J. 2003. Smart and genetically engineered biomaterials and drug delivery systems. *European journal of pharmaceutical sciences*, 20(1):1-16.
- Kopeček, J. 2013. Polymer–drug conjugates: origins, progress to date and future directions. *Advanced drug delivery reviews*, 65(1):49-59.



- Kumar, A. 2013. Development and Characterization of Ribavirin Loaded Poly (Lactide-Co-Glycolide) Nanoparticles by Double Emulsification Method.
- Kumari, A., Yadav, S.K. & Yadav, S.C. 2010. Biodegradable polymeric nanoparticles based drug delivery systems. *Colloids and Surfaces B: Biointerfaces*, 75(1):1-18.
- Langer, R. 1993. Polymer-controlled drug delivery systems. *Accounts of chemical research*, 26(10):537-542.
- Lembo, D. & Cavalli, R. 2010a. Nanoparticulate delivery systems for antiviral drugs. *Antivir Chem Chemother*, 21(2):53-70.
- Lembo, D. & Cavalli, R. 2010b. Nanoparticulate delivery systems for antiviral drugs. *Antiviral Chemistry and Chemotherapy*, 21(2):53-70.
- Lepeltier, E., Bourgaux, C. & Couvreur, P. 2014. Nanoprecipitation and the “Ouzo effect”: Application to drug delivery devices. *Advanced drug delivery reviews*, 71:86-97.
- Li, L., Wang, H., Ong, Z.Y., Xu, K., Ee, P.L.R., Zheng, S., et al. 2010. Polymer- and lipid-based nanoparticle therapeutics for the treatment of liver diseases. *Nano Today*, 5(4):296-312.
- Li, X., Wu, Q., Chen, Z., Gong, X. & Lin, X. 2008. Preparation, characterization and controlled release of liver-targeting nanoparticles from the amphiphilic random copolymer. *Polymer*, 49(22):4769-4775.
- Liu, J., Xiao, Y. & Allen, C. 2004. Polymer–drug compatibility: a guide to the development of delivery systems for the anticancer agent, ellipticine. *Journal of pharmaceutical sciences*, 93(1):132-143.
- Logothetidis, S. 2012. Nanomedicine and nanobiotechnology: Springer Science & Business Media.

Marques, M.R.C., Loebenberg, R., Almukainzi, M. 2011. Simulated biological fluids with possible application in dissolution testing.

Messina, J.P., Humphreys, I., Flaxman, A., Brown, A., Cooke, G.S., Pybus, O.G., et al. 2015. Global distribution and prevalence of hepatitis C virus genotypes. *Hepatology*, 61(1):77-87.

Moghimi, S.M., Hunter, A.C. & Murray, J.C. 2001. Long-circulating and target-specific nanoparticles: theory to practice. *Pharmacological reviews*, 53(2):283-318.

Morales-Cruz, M., Flores-Fernández, G.M., Morales-Cruz, M., Orellano, E.A., Rodriguez-Martinez, J.A., Ruiz, M., et al. 2012a. Two-step nanoprecipitation for the production of protein-loaded PLGA nanospheres. *Results in pharma sciences*, 2:79-85.

Morales-Cruz, M., Flores-Fernández, G.M., Morales-Cruz, M., Orellano, E.A., Rodriguez-Martinez, J.A., Ruiz, M., et al. 2012b. Two-step nanoprecipitation for the production of protein-loaded PLGA nanospheres. *Results in Pharma Sciences*, 2:79-85.

Nagavarma B V N, H.K.S.Y., Ayaz A, Vasudha L.S, Shivakumar H.G. 2012. Different techniques for preparation of polymeric nanoparticles a review. *Asian Journal of Pharmaceutical and Clinical Research*, 5(20 June 2012):8.

Nagavarma, B., Yadav, H.K., Ayaz, A., Vasudha, L. & Shivakumar, H. 2012. Different techniques for preparation of polymeric nanoparticles—a review. *Asian J. Pharm. Clin. Res*, 5(3):16-23.

Nidhin, M., Indumathy, R., Sreeram, K.J. & Nair, B. 2008. Synthesis of iron oxide nanoparticles of narrow size distribution on polysaccharide templates. *Bulletin of Materials Science*, 31(1):93-96.

Nishimata, S., Tsutsumi, N., Suzuki, S., Nagao, R., Kashiwagi, Y. & Kawashima, H. 2014. Efficacy of re-treatment by peginterferon alpha-2a and ribavirin in a child with hepatitis C. *Journal of Infection and Chemotherapy*, 20(7):443-445.

- Overhoff, K.A., McConville, J.T., Yang, W., Johnston, K.P., Peters, J.I. & Williams, R.O. 2008. Effect of stabilizer on the maximum degree and extent of supersaturation and oral absorption of tacrolimus made by ultra-rapid freezing. *Pharmaceutical Research*, 25.
- Owens Iii, D.E. & Peppas, N.A. 2006. Opsonization, biodistribution, and pharmacokinetics of polymeric nanoparticles. *International Journal of Pharmaceutics*, 307(1):93-102.
- Oze, T., Hiramatsu, N., Yakushijin, T., Mochizuki, K., Oshita, M., Hagiwara, H., et al. 2011. Indications and limitations for aged patients with chronic hepatitis C in pegylated interferon alfa-2b plus ribavirin combination therapy. *Journal of hepatology*, 54(4):604-611.
- Panyam, J. & Labhasetwar, V. 2003. Biodegradable nanoparticles for drug and gene delivery to cells and tissue. *Advanced drug delivery reviews*, 55(3):329-347.
- Panyam, J. & Labhasetwar, V. 2012. Biodegradable nanoparticles for drug and gene delivery to cells and tissue. *Advanced drug delivery reviews*, 64, Supplement:61-71.
- Patterson, J.L. & Fernandez-Larsson, R. 1990. Molecular mechanisms of action of ribavirin. *Review of Infectious Diseases*, 12(6):1139-1146.
- Pawlotsky, J.M., Chevaliez, S. & McHutchison, J.G. 2007. The Hepatitis C Virus Life Cycle as a Target for New Antiviral Therapies. *Gastroenterology*, 132(5):1979-1998.
- Pillai, O. & Panchagnula, R. 2001. Polymers in drug delivery. *Current opinion in chemical biology*, 5(4):447-451.
- Pinto Reis, C., Neufeld, R.J., Ribeiro, A.J. & Veiga, F. 2006. Nanoencapsulation I. Methods for preparation of drug-loaded polymeric nanoparticles. *Nanomedicine: Nanotechnology, Biology and Medicine*, 2(1):8-21.
- Raval, A., Parikh, J. & Engineer, C. 2010. Mechanism of controlled release kinetics from medical devices. *Brazilian Journal of Chemical Engineering*, 27(2):211-225.

- Reddy, K.R., Nelson, D.R. & Zeuzem, S. 2009. Ribavirin: current role in the optimal clinical management of chronic hepatitis C. *Journal of hepatology*, 50(2):402-411.
- Redhead, H.M., Davis, S.S. & Illum, L. 2001. Drug delivery in poly(lactide-co-glycolide) nanoparticles surface modified with poloxamer 407 and poloxamine 908: in vitro characterisation and in vivo evaluation. *Journal of Controlled Release*, 70(3):353-363.
- Reis, C.P., Neufeld, R.J., Ribeiro, A.J. & Veiga, F. 2006. Nanoencapsulation I. Methods for preparation of drug-loaded polymeric nanoparticles. *Nanomedicine: Nanotechnology, Biology and Medicine*, 2(1):8-21.
- Roberts, M.J., Bentley, M.D. & Harris, J.M. 2002. Chemistry for peptide and protein PEGylation. *Advanced drug delivery reviews*, 54(4):459-476.
- Shepard, C.W., Finelli, L. & Alter, M.J. 2005. Global epidemiology of hepatitis C virus infection. *The Lancet infectious diseases*, 5(9):558-567.
- Sun, T., Zhang, Y.S., Pang, B., Hyun, D.C., Yang, M. & Xia, Y. 2014. Engineered nanoparticles for drug delivery in cancer therapy. *Angewandte Chemie International Edition*, 53(46):12320-12364.
- Takaki, S., Tsubota, A., Hosaka, T., Akuta, N., Someya, T., Kobayashi, M., et al. 2004. Factors contributing to ribavirin dose reduction due to anemia during interferon alfa2b and ribavirin combination therapy for chronic hepatitis C. *Journal of gastroenterology*, 39(7):668-673.
- Uhrich, K.E., Cannizzaro, S.M., Langer, R.S. & Shakesheff, K.M. 1999. Polymeric systems for controlled drug release. *Chemical reviews*, 99(11):3181-3198.
- Van Vlierberghe, H., Delanghe, J., De Vos, M. & Leroux-Roel, G. 2001. Factors influencing ribavirin-induced hemolysis. *Journal of hepatology*, 34(6):911-916.
- Verma, A. & Stellacci, F. 2010. Effect of surface properties on nanoparticle–cell interactions. *Small*, 6(1):12-21.

World Health Organization. (2013). Global policy report on the prevention and control of viral hepatitis in WHO member states. WHO Library Cataloguing-in-Publication Data.

World Health Organisation. 2014. Hepatitis C factsheet [online].Available from: <http://who.int/mediacentre/factsheets/fs164/en/>[accessed 24 August 2014]

Zhang, X.-Z., Zhuo, R.-X., Cui, J.-Z. & Zhang, J.-T. 2002. A novel thermo-responsive drug delivery system with positive controlled release. *International journal of pharmaceutics*, 235(1):43-50.

Zhu, B., Liu, G.-L., Ling, F. & Wang, G.-X. 2015. Carbon nanotube-based nanocarrier loaded with ribavirin against grass carp reovirus. *Antiviral research*, 118:29-38.